Food and Bioprocess Technology (2023) 16:1851–1872
https://doi.org/10.1007/s11947-023-03008-1

RESEARCH

Chitosan-Based Nanoencapsulation of *Ocimum americanum* Essential Oil as Safe Green Preservative Against Fungi Infesting Stored Millets, Aflatoxin B_1 Contamination, and Lipid Peroxidation

Bijendra Kumar Singh[1,3] · Shikha Tiwari[1] · Akash Maurya[1] · Somenath Das[2] · Vipin Kumar Singh[4] · Nawal Kishore Dubey[1]

Received: 3 April 2022 / Accepted: 19 January 2023 / Published online: 28 February 2023

Abstract

Present study deals with the first-time report on encapsulation of *Ocimum americanum* essential oil (OAEO) into chitosan matrix with enhanced antifungal, aflatoxin B_1 (AFB_1) inhibition, antioxidant activity, and in situ efficacy in the millet food system. GC–MS analysis suggested citral (66.72%) as the major component of OAEO. Physicochemical characterizations through SEM, FTIR, and XRD analyses confirmed the successful loading of OAEO into chitosan nanoemulsion (OAEO-CsNe). In vitro release profile of nanoencapsulated OAEO exhibited biphasic burst and controlled volatilisation, a prerequisite for long-term antifungal effect in the stored food system. OAEO-CsNe completely inhibited the growth and AFB_1 production of *Aspergillus flavus* at 0.2 and 0.175 µL/mL, respectively. Inhibition of ergosterol biosynthesis followed by the release of vital cellular ions, and 260, 280 nm absorbing materials from AFLHPSi-1 cells suggested plasma membrane as a potential site of antifungal action of OAEO-CsNe. Significant reduction of cellular methylglyoxal (an AFB_1 inducer) level in AFLHPSi-1 cells after fumigation with OAEO-CsNe confirmed the novel biochemical mechanism of anti-aflatoxigenic activity. Additionally, in silico modelling of citral (major component of OAEO) with Ver-1 and Omt-A proteins suggested the hydrogen bond-dependent molecular interaction for inhibition of AFB_1 biosynthesis. OAEO-CsNe showed significant in situ antifungal, anti-aflatoxigenic, and lipid peroxidation-suppressing potentialities without altering the organoleptic and germination properties of *Setaria italica* seeds. Moreover, the appreciative safety profile (LD_{50} = 11,162.06 µL/kg) of OAEO-CsNe in a mammalian model system (*Mus musculus*) strengthens its recommendation as an effective green preservative against fungal infestation, AFB_1 contamination, and reactive oxygen species-mediated lipid peroxidation in stored food commodities.

Keywords *Ocimum americanum* essential oil · *Setaria italica* · Aflatoxin B_1 · Nanoencapsulation · In situ efficacy · In silico modelling

Introduction

Despite of substantial advancements in contemporary food processing technology, moulds and mycotoxins contamination in different agricultural commodities during storage periods is an unavoidable challenge across the world even in the twenty-first century. Mycotoxins, which are toxic secondary metabolites of fungal species generally belonging to the genera *Aspergillus*, *Penicillium*, and *Fusarium*, commonly contaminate the cereals and food grain products (Alshannaq & Yu, 2017; Jafarzadeh et al., 2022; Nada et al., 2022). Fungal infestation and mycotoxin contamination in stored food commodities obstruct the normal synthesis of different biomacromolecules such as nucleic acids and proteins, resulting in the emergence of various health problems (Kos et al.,

✉ Nawal Kishore Dubey
nkdubeybhu@gmail.com

1 Laboratory of Herbal Pesticides, Centre of Advanced Study (CAS) in Botany, Institute of Science, Banaras Hindu University, Varanasi 221005, India

2 Department of Botany, Burdwan Raj College, Purba Bardhaman, West Bengal, Bardhaman 713104, India

3 Department of Botany, Feroze Gandhi College, Raebareli 229001, India

4 Department of Botany, K. S. Saket P. G. College, Ayodhya 224123, India

2020). Among different reported mycotoxins, Aflatoxin B_1 represents a serious threat to humans and animals due to their carcinogenic, teratogenic, mutagenic, and immunosuppressive activities and more importantly classified under Class 1 human carcinogen (International Agency for Research on Cancer, 2012; Ostry et al., 2017).

Millets are small-seeded crops of the grass family (Poaceae) used as staple foods in many African and Asiatic countries, and recently their novel function in gut health promotion has been reported due to the availability of a variety of nutritional components and dietary fibres (Wani et al., 2021). The *Setaria italica* L. (foxtail millet) is one of the world's oldest millet crops with the highest yielding grain, and accounting for a significant portion of worldwide economic output and extensively cultivated in the developing countries, semiarid and arid regions of Africa, Americas, and Asia (Lata et al., 2013; Sharma & Niranjan, 2018). Kola et al. (2020) reported an abundance occurrence of minerals such as calcium, zinc, iron, manganese, potassium, copper, and phosphorus in *S. italica* seeds, suggesting their importance as a functional food. However, fungal infestation and mycotoxin contamination in stored millets is a severe problem all over the world. Millets' vulnerability to toxigenic fungus during storage, in addition to mycotoxin enrichment, causes deterioration of nutritional and sensory qualities (Choi et al., 2021). Moreover, lipid peroxidation in stored food causes the production of reactive oxygen species (ROS), which triggers the synthesis of cellular methylglyoxal (MG), which is considered as prime AFB_1 inducer in foods (Ju et al., 2020; Upadhyay et al., 2021).

Different synthetic preservatives have been employed to reduce fungal and AFB_1 contamination; however, indiscriminate use of such synthetic compounds has resulted in the development of resistance races among innumerable fungal populations, toxicity to non-target organisms, and loss of environmental sustainability (Ali et al., 2018; OuYang et al., 2020). Currently, plant essential oils (EOs) are increasingly being investigated as alternative control strategies (Das et al., 2021a; Papoutsis et al., 2019). Although EOs display tremendous food preservative potentialities against fungal infestation and AFB_1 contamination, however, their large-scale practical application is limited due to volatility, oxidative degradation, shorter shelf life, intense aroma, and interaction with food matrix under variable environmental conditions (Ghaderi-Ghahfarokhi et al., 2016; Yang et al., 2022). Nanotechnology is one of the most quickly evolving technologies, with unique uses of diverse nanomaterials in agriculture and the food industries. To prevent the undesirable effect of EO, nanoencapsulation into suitable food-grade biopolymers is desired, resulting into the formation of small-sized nanoemulsion with enhanced efficacy, improved shelf-life, and controlled release behaviour (Plati & Paraskevopoulou, 2022; Saeed et al., 2022; Singh et al., 2021). Among different natural polymers, chitosan has been widely used owing to its greater availability, biodegradability, cost-effectiveness, antimicrobial property, GRAS status, high encapsulation efficiency, and antioxidant activities (Maleki et al., 2022; Wani et al., 2022). Among different reported process of nanoencapsulation, ionic gelation has been claimed to be a superior approach for producing chitosan-loaded EO release systems due to its moderate experimental conditions, non-organic solvents utilizations, innoxious qualities, and controlled nature, hence, widely employed in different food, agricultural, and pharmaceutical industries (Elsaied & Tayel, 2022; Singh et al., 2022). The electrostatic interaction between the ammonium group of chitosan and the phosphate groups of sodium-tripolyphosphate (S-TPP) is the basis for the synthesis EO loaded chitosan nanoparticles (Cai et al., 2022; Esmaeili & Asgari, 2015).

Ocimum americanum L. (Family: Lamiaceae) commonly known as lime basil, hoary basil, and American basil is an annual herb native to Africa, Indian subcontinent, China, and Southeast Asia with a distinct mint flavour, and hairy leaves with scented flowers (Giri, 2019; Sarma & babu, 2011; Shadia et al., 2007; Simon et al., 1999). The EO of *O. americanum* (OAEO) obtained from the aerial parts through hydro-distillation showed prominent antibacterial and antifungal activities (da Silva et al., 2018; Hassane et al., 2012). However, the reports regarding the antifungal activity of OAEO against millet contaminating fungi along with AFB_1 inhibition and improvement in overall biological efficacy through nanoencapsulation of OAEO into chitosan matrix for shelf-life extension are completely lacking.

Therefore, the objective of the present investigation was an encapsulation of chemically characterised OAEO into chitosan nanomatrix, physico-chemical characterization, and estimation of antifungal and anti-aflatoxigenic activities in stored millets. Moreover, the investigation sheds light on biochemical and molecular mechanisms of antifungal and antiaflatoxigenic activities involving different cellular targets like ergosterol, methylglyoxal, and AFB_1 synthesising protein Ver-1 and Omt-A with an aim to fill the knowledge gap of previous investigations on EOs and nanoformulations for protection of stored food system against fungal infestation and AFB_1 contamination. More importantly, millets, especially *S. italica* seeds is a commodity of great economical, medical, and pharmaceutical importance due to its tremendous minerals and fibre content (super food); hence, preservation of in situ nutritional quality of millets in the storage conditions is an important parameter of the study. Additionally, in situ antifungal activity, AFB_1 inhibition and lipid peroxidation suppressing potentialities along with phytotoxicity analysis, sensorial properties, and safety profile assessment were also performed in stored *S. italica* (as a model millet food system) seeds to strengthen the application of encapsulated

OAEO nanoemulsion as a safe and green preservative in food and agricultural industries.

Material and Methods

Materials

Chitosan powder (deacetylation degree > 90%), dichloromethane (CH_2Cl_2), acetic acid (99.99% purity), sodium tripolyphosphate (S-TPP), chloroform, Tween-80, Tween-20, 2,2′-azino-bis (3-ethylbenzothiazoline-6-sulfonic acid) (ABTS), 1,1- diphenyl-2-picrylhydrazyl (DPPH), 1,2-diaminobenzene (DAB), thiobarbeturic acid (TBA), sodium carbonate, trichloroacetic acid (TCA), perchloric acid ($HClO_4$), potassium carbonate, methylglyoxal, nutrient media PDA (Dextrose—20 g/L, Agar—15 g/L, and potato infusion powder—200 g/L), SMKY (Sucrose—200 g/L, $MgSO_4.7H_2O$—0.5 g/L, KNO_3—0.3 g/L, Yeast extract—7.0 g/L) were purchased from Hi-Media laboratories, Mumbai, India.

Culture Condition and Fungal Strain Used

The aflatoxigenic strain of *A. flavus* (AFLHPSi-1) was isolated during mycobiota analysis of different millet samples (*S. italica*, *Panicum sumatrense*, and *Paspalum scrobiculatum*) from our previous investigation and used for the present investigation.

Isolation and Chemical Profiling of OAEO

Aerial parts of *O. americanum* were collected from the nearby locality of Handia, Prayagraj, India, and identified by Prof N. K. Dubey, Department of Botany, Banaras Hindu University, Varanasi, India. The fresh plant parts (500 g) were washed with distilled water and kept in Clevenger's apparatus for oil extraction through hydrodistillation for 4 h. Anhydrous sodium sulphate was used to absorb extra traces of water. The collected OAEO was kept in an amber vial at 4 °C for further utilisation in the experiment. Yield of OAEO was calculated based on the weight of plant parts used by the following formula (1).

$$OAEO\ Yield\ (mL/kg) = \frac{\text{Volume of extracted EO (mL)}}{\text{Weight of plant parts utilised for extraction (kg)}} \quad (1)$$

The chemical profiling of OAEO was done through GC–MS (GC: Thermo scientific 1300 GC and MS: Perkin Elmer Turbomass Gold MA, USA) analysis equipped with TG-5 capillary column of 30 m × 0.25 mm ID × 0.25 µm thickness and temperature of instrument programmed from 60 to 240 °C at the rate of 5 °C/min. One microlitre of OAEO (1000 times diluted in acetone) was injected into the column and the splitting ratio was kept as 1:50. Helium was used as carrier gas; transfer line temperature and oven temperatures were regulated according to standard protocol (Adams, 2007). The components were identified by retention times, percent area with respect to the spectral peaks of reference compounds reported in libraries such as NIST, NBS, Wiley, and FFNSC-2 database along with other data published in the literature.

Synthesis of Chitosan-OAEO Nanoemulsion

The method of Yoksan et al. (2010) was adapted for the synthesis of chitosan-OAEO nanoemulsion with slight modifications. 20 mL of chitosan solution (1.5%) was prepared in 1% acetic acid by overnight agitation in a magnetic stirrer followed by dropwise addition of Tween-80 as surfactant and stirred at 45 °C for 2 h. Requisite amounts of OAEO (0.06, 0.12, 0.18, 0.24, and 0.30 g) were diluted in 4 mL of CH_2Cl_2 and added dropwise in 20 mL of chitosan solution during homogenization at 13,000 rpm for 10 min in an ice bath. Thereafter, 20 mL of S-TPP (0.4% w/v) solution was added dropwise with a dropping funnel and stirred for 45 min at room temperature. Nanoemulsion was collected after centrifugation (REMI compufuge CPR-4) at 13, 000 rpm for 10 min at 4 °C and washing with 0.1% Tween-20 solution. Similar procedure was performed for the synthesis of chitosan nanoemulsion (CsNe) without using OAEO. The varying proportions of chitosan and OAEO (w/v), i.e. 1:0.0, 1:0.2, 1:0.4, 1:0.6, 1:0.8, and 1:1 was synthesised and tested for improved loading characteristics.

Loading Capacity and Encapsulation Efficiency of OAEO-CsNe

The loaded capacity OAEO into chitosan nanomatrix was determined by UV–Visible spectroscopy (UV-2600, Shimadzu, Japan). Absorbance maxima of OAEO were obtained in ethyl acetate at 258 nm ($y = 0.0106\times + 0.0377$; $R^2 = 0.9991$). For this, 300 µL aliquot of OAEO nanoemulsion was dissolved into 3 mL of ethyl acetate, mixed properly followed by centrifugation (REMI compufuge CPR-4) at 13,000 g for 10 min. The absorbance of obtained supernatant was recorded at 258 nm for determination of encapsulation efficiency (EE) and loading capacity (LC) by using Eqs. 2 and 3 respectively.

$$\%EE = \frac{\text{Amount of loaded OAEO}}{\text{Initial amount of OAEO added}} 100 \quad (2)$$

$$\%LC = \frac{\text{Amount of loaded OAEO in nanoemulsion}}{\text{Amount of OAEO added}} 100 \quad (3)$$

The percent nanoencapsulation yield (NY) was determined from the total dry weight of lyophilised nanoparticles and the total dry weight of individual constituents used during nanoparticle synthesis.

% NY = Lyophilised nanoparticles weight/Total dry weight of initial constituents × 100

$$\%NY = Lyophilised\ nanoparticles\ weight / Total\ dry\ weight\ of\ initial\ constituents \times 100 \quad (4)$$

Characterization of Synthesised Nanoemulsions (OAEO-CsNe)

Determination of Morphology Through Scanning Electron Microscope (SEM)

The morphological appearances of synthesised nanoemulsions (CsNe and OAEO-CsNe) were determined through a scanning electron microscope (SEM) (Evo-18 researcher, Zeiss, Germany). For this, 200 µL of CsNe and OAEO-CsNe were dissolved in 10 of DDW, sonicated, and 10 µL of prepared aliquot was dropped on cover glass, spread uniformly to form a thin film. The dried films were coated with gold and examined under SEM.

Fourier Transform Infrared (FTIR) Spectroscopy

The FTIR spectra were recorded for chitosan powder (CsP), OAEO, powdered CsNe, and OAEO-CsNe by Perkin Elmer IR spectrometer (USA). The samples were mixed with KBr to form thin pellets prior to analysis under 64 scans at a resolution of 4 cm^{-1} from 500 to 4000 cm^{-1}.

X-Ray Diffractometry (XRD) Study

The effect of OAEO nanoencapsulation on the relative crystallinity of chitosan X-ray diffractometer (Bruker D8 Advance) was used to analyse the crystallographic profiles of CsP, CsNe, and AREO-CsNe. The measurement was done over the 2θ range from 5 to 50° with a step angle of 0.02° min^{-1} and scanned speed of 5° min^{-1}.

In Vitro Release Assay

The method of Hasheminejad et al. (2019) with slight modification was applied for the determination of the in vitro release profile of OAEO from chitosan nanoemulsion. The cumulative content of OAEO released into phosphate buffer saline (pH 7.4) was analysed at specific time intervals (8 to 152 h) by UV–visible spectrophotometer (UV-2600, Shimadzu, Japan) at 258 nm, and Eq. (5) was taken into consideration for calculating % cumulative release of OAEO.

$$\%\text{Cumulative release of } OAEO = \frac{\text{Cumulative amount } of \text{ OAEO released at each time}}{\text{Initial amount of OAEO loaded in the sample}} \times 100 \quad (5)$$

Antifungal and Anti-Aflatoxigenic Activities of OAEO and OAEO-CsNe

Requisite amounts of OAEO (0.05–0.4 µL/mL) and OAEO-CsNe (0.025–0.2 µL/mL) were mixed separately with 25 mL SMKY medium in a conical flask to achieve the desired concentrations. Two different control sets were prepared by adding 500 µL of 0.5% Tween 20 for OAEO and CsNe for OAEO-CsNe, respectively. All the sets were inoculated with 25 µL spore suspension of AFLHPSi-1 (density = 10^6 spores/mL) strain and kept at 27 ± 2 °C in BOD incubator for 10 days. The lowest concentration of OAEO and OAEO-CsNe causing complete inhibition of AFLHPSi-1 growth was recorded as minimum inhibitory concentrations (MICs).

The AFB_1 inhibitory efficacy of OAEO and OAEO-CsNe was determined in terms of minimum AFB_1 inhibitory concentration (MAIC). For MAIC estimation, the content of 10 days old cultured isolates (treated with different concentrations of OAEO and OAEO-CsNe) were filtered through Whatman no. 1 paper, and the filtrate was mixed properly with 20 mL chloroform in a separating funnel followed by evaporation on a water bath (80 °C) till complete evaporation and residues were re-dissolved in 1 mL of cold methanol. Methanolic extract (50 µL) was spotted on a silica gel G plate, and developed in a solvent comprising of toluene: isoamyl alcohol: methanol, 90:32:2 (v/v/v), followed by observation under UV transilluminator (Zenith, India). The blue-coloured spots represented the presence of AFB_1, and scrapped spots were dissolved in 5 mL methanol and centrifuged for 10 min at 5000 g. The absorbance of the collected supernatant was recorded at 360 nm using UV–visible spectrophotometry (UV-2600, Shimadzu, Japan) and the concentration of AFB_1 was estimated using the Eq. (6) (Tian et al., 2012).

$$\text{AFB1 content } \left(\frac{\mu g}{mL}\right) = \frac{DM}{EL} \times 1000 \quad (6)$$

where D = absorbance, M = molecular weight of AFB_1 (312), E = molar extinction coefficient of AFB_1 (21,800), and L = path length (1 cm).

Mode of Action

Effect of OAEO and OAEO-CsNe on Membrane Ergosterol Level of AFLHPSi-1 Cells

The ergosterol content was estimated by the methodology of Tian et al. (2012) with slight modifications. Different concentrations of OAEO (0.05–0.4 µL/mL), and OAEO-CsNe (0.025–0.2 µL/mL) were added to 25 mL SMKY medium in conical flasks and inoculating with 25 µL of AFLHPSi-1 spore suspension followed by incubation in BOD incubator at 27 ± 2 °C for 7 days. Control sets were devoid of OAEO and OAEO-CsNe addition in the SMKY medium. After completion of incubation periods, fungal mat from all sets was autoclaved, washed with distilled water, soaked in blotting paper, and weighed. Fungal biomass was mixed with 5 mL of 25% ethanolic KOH solution in culture tubes, vortexed for 3 min, followed by incubation in a water bath at 70 °C for 2 h. Thereafter, 2 mL of distilled water and 5 mL of n-heptane were added to the fungal biomass, and again vortexed for 3 min. The samples were incubated at room temperature for 1–2 h, and the upper layer of n-heptane was analysed between 230 and 300 nm using a UV–visible spectrophotometer (UV-2600, Shimadzu, Japan). The content of ergosterol in samples was calculated by following Eq. (7) described by Kedia et al. (2014).

% Ergosterol = *A* (% ergosterol + % 24 (28) dehydroergosterol) − *B* (% 24 (28) dehydroergosterol).

$$B(\%24(28)\ dehydroergosterol) = Abs.230/518)/pellet\ weight \quad (7)$$

A (% ergosterol + % 24 (28) dehydroergosterol) = (Abs.282/290)/ pellet weight.

B (% 24 (28) dehydroergosterol) = (Abs.230/518)/ pellet weight. (7).

where, 290 and 518 are the *E* values in percent/cm determined for crystalline ergosterol and 24 (28) dehydroergosterol and pellet weight (g).

Estimation of Cellular Constituent's Release

The effect of OAEO and OAEO-CsNe on membrane damage was estimated in terms of the release of vital cellular cations (Ca^{2+}, Mg^{2+}, and K^{+}) and 260, 280 nm absorbing materials from AFLHPSi-1 cells following the protocol of Deepika et al. (2021) with slight modifications. Biomass of 7-day-old culture of AFLHPSi-1 cells was washed with double distilled water and suspended in 20 mL of 0.85% saline solution, followed by fumigation with different concentrations of OAEO (0.05–0.4 µL/mL), and OAEO-CsNe (0.025–0.2 µL/mL). Control sets were prepared without the addition of OAEO and OAEO-CsNe. Both control and treatment sets were incubated at 27 ± 2 °C in a BOD incubator for overnight. After the incubation period, the fumigated fungal biomass was filtered; supernatant was utilised for analysis of leakage of cellular cations by atomic absorption spectrometry (PerkinElmer, AAnalyst 800, USA). The absorbance of filtrate at 260 and 280 nm was recorded by UV–Visible spectrophotometer (UV-2600, Shimadzu, Japan) to determine the leakage of 260 and 280 nm absorbing materials from the AFLHPSi-1 cells.

Effect of OAEO and OAEO-CsNe on Methylglyoxal (MG) Content of AFLHPSi-1 Cells

For the estimation of cellular methylglyoxal in AFLHPSi-1 cells, the methodology of Upadhyay et al. (2018) was used with some modifications. Six- to seven-days-old fungal biomass of AFLHPSi-1 was harvested and 300 mg was transferred to 10 mL of SMKY medium and fumigated with different concentration of OAEO (0.05–0.4 µL/mL), and OAEO-CsNe (0.025–0.2 µL/mL). Control sets were prepared without the addition of OAEO and OAEO-CsNe. Control and treatment sets were placed in a BOD incubator at 27 ± 2 °C for overnight. Thereafter, the fungal biomass was washed with distilled water and crushed in 3 mL of 0.5 M perchloric acid in cold chamber conditions and placed in an ice bath for 15 min. Crushed biomass was centrifuged (Remi compufuge CPR-4, India) at 13,000 × g for 10 min at 4 °C and the supernatant was neutralised by a saturated solution of potassium carbonate, followed by again centrifugation, and collection of supernatants. For estimation of cellular methylglyoxal, 250 µL of 1, 2-diaminobenzene (7.2 mM), 100 µL of perchloric acid (5 M), and 650 µL of neutralised supernatant was added and incubated for 30 min at 25 ± 2 °C. Thereafter, the absorbance of the samples was recorded at 336 nm (Yadav et al., 2005). The absorbance was compared with the standard curve obtained by pure MG (10–100 µM) and the level of MG estimated in fumigated cells.

In Silico Molecular Modelling of Citral with Ver-1 and Omt-A Proteins for AFB_1 Inhibition

The three-dimensional structure of citral (major component of OAEO) was downloaded from PubChem online data base in SDF format. Ver-1 and Omt-A (AFB_1-producing proteins) were downloaded from the UniProt website in FASTA format and proteins were modelled by the help of the Phyre 2 online server. The molecular interactions of major component citral with Ver-1 and Omt-A proteins were performed by using UCSF Chimera software. Further, the binding/interaction of citral with Ver-1 and Omt-A proteins was selected on the basis of binding energy (Kcal/mol) and number of hydrogen bonds present between them (Prasad et al., 2022).

Determination of Total Phenolic Content and Free Radical Scavenging Activity

The total phenolic content of OAEO and OAEO-CsNe was determined by using Folin ciocalteu's reagent following the calorimetric method of Gholivand et al. (2010) with slight modifications. The total amount of phenolic content was quantified in µg gallic acid equivalent to per mg of OAEO by using the following Eq. (8)

$$Absorbance = 0.0012 \times gallicacid + 0.024 \quad (8)$$

Free radical scavenging activities of OAEO and OAEO-CsNe were determined by $DPPH^{\bullet+}$ and $ABTS^{\bullet+}$ assay. For $DPPH^{\bullet+}$ assay, different concentrations of OAEO and OAEO-CsNe (5–50 µL/mL) were added in 0.004% methanolic solution of $DPPH^{\bullet+}$ (prepared before 12 h and kept in a dark condition), incubated at room temperature for 30 min, and absorbance was recorded at 517 nm using methanolic $DPPH^{\bullet+}$ solution as blank. For $ABTS^{\bullet+}$ assay, the reaction mixture was prepared by mixing equal volumes of 7 mM $ABTS^{\bullet+}$ stock solution with 140 mM of potassium persulphate and kept at room temperature under dark condition for 12–14 h (Re et al., 1999). The prepared mixture was diluted with ethanol until absorbance maintained at 0.7 ± 0.05 nm. Different concentrations of OAEO and OAEO-CsNe (2–20 µL/mL) were added to $ABTS^{\bullet+}$ mixture and absorbance of the samples was recorded at 734 nm after 6 min of the incubation period. The % scavenging activities of OAEO and OAEO-CsNe were measured in terms of IC_{50} values, which were calculated from the graph plotted between % radical scavenging and concentrations of OAEO and OAEO-CsNe. % Free radical scavenging activity was calculated by following Eq. (9).

$$\%\text{Inhibition} = \frac{A\text{blank} - A\text{sample}}{A\text{blank}} \times 100 \quad (9)$$

where A blank = absorbance of blank.

A sample = absorbance of solution containing different concentrations of samples.

In Situ Efficacy of OAEO and OAEO-CsNe: HPLC Analysis in *S. italica* Seeds

The effectiveness of OAEO and OAEO-CsNe against AFL-HPSi-1 was tested in *S. italica* seeds that had been kept in sealed containers for a year. The millets seeds were fumigated with MIC dosages of OAEO (0.4 µL/mL) and OAEO-CsNe (0.2 µL/mL) in set one of the experiments. Seeds were fumigated with 2MIC dosages of OAEO (0.8 µL/mL) and OAEO-Cs-Ne (0.4 µL/mL) in set two. Set three was used as a control, containing millets seeds that had not been treated with OAEO or OAEO-CsNe. For 1 year, all of the sets were kept at 25 ± 2 °C and 70% relative humidity. The samples were processed and evaluated for AFB_1 contamination using high-performance liquid chromatography (HPLC), once the storage time was completed.

In a nutshell, 10 g of finely powdered materials were blended with 10 mL mixture of methanol and distilled water (8:10 v/v), shaken for 30 min, then centrifuged for 10 min at 5000 g. 4 mL supernatant was combined with 300 µL chloroform and 6 mL distilled water containing 3% KBr and centrifuged one more time. The collected settled phase was evaporated in a water bath and dissolved in 500 µL of HPLC-grade methanol. The mobile phase of methanol, acetonitrile, and distilled water (17:19:64 v/v/v) was used to inject 50 µL of sample into a C-18 reverse phase column. The amount of AFB_1 in *S. italica* seeds was measured in µg/kg.

Estimation of Lipid Peroxidation in Stored *S. italica* Seeds

Lipid peroxidation estimation in *S. italica* seeds treated with OAEO and OAEO-CsNe (MIC and 2 MIC doses) was done using thiobarbituric acid (TBA) assay following Das et al. (2020). Stored seeds without fumigation of EO and emulsion were considered as control. For this, 0.5 g grinded seed samples were mixed with a 4 mL reaction mixture (15% TCA, 0.375% TBA, and 0.25 N HCl) followed by heating on a water bath for 15 min at 70 °C. The mixture was centrifuged at 12,000 g for 10 min and the absorbance of obtained supernatant was recorded at 532 and 600 nm, respectively. The MDA content of samples was calculated using the molar extinction coefficient (0.155 μM^{-1} cm^{-1}) and expressed in terms of µM/gFW of stored seeds.

Safety Profile Assessment of OAEO and OAEO-CsNe in Mice

The safety profile assessment of OAEO and OAEO-CsNe was inspected on male mice (*Mus musculus* L., average weight 30 g and 3 months old) through acute oral toxicity and LD_{50} values was determined with the help of Probit analysis. Before conducting an experiment, permission from the Animal care and Ethical committee of BHU was taken and mice were acclimatised for 7 days under laboratory conditions. Different concentrations of OAEO (100–500 µL) and OAEO-CsNe (100–1000 µL) were orally administered through a micropipette catheter to each group of the mice. For control sets, Tween-20 and CsNe were administered to the mice group. All groups were monitored periodically between 4 and 24 h and at the end of the observation period, a number of dead mice were counted for determining LD_{50} by Probit analysis (Finney, 1971). After completion of the experiment, mice were sacrificed.

Phytotoxicity Assay of OAEO and OAEO-CsNe Fumigated *S. italica* Seeds

Phytotoxicity assay of stored *S. italica* seeds (fumigated and non-fumigated) was done through the emergence of plumule and radicles through seed germination assay. Stored seeds were washed with distilled water, and placed in Petri plates containing moistened blotting paper. The length of plumule and radicle were measured at regular time interval by centimetre scale.

Sensory Profile Assessment of OAEO and OAEO-CsNe Fumigated *S. italica* Seeds

Sensory profile assessment of fumigated *S. italica* seeds was carried out with a group of ten people of both genders (22 to 50 years) and were asked to assess the colour, texture, flavour, mouth feel, and overall acceptability on a five-point hedonic scale (5 = extremely acceptable, 4 = slightly acceptable, 3 = moderately acceptable, 2 = acceptable, and 1 = not acceptable). Samples were provided in packets and coded with arbitrary digits to the participants.

Statistical Analysis

All the experiments were performed in a set of three. Data analysis was performed on mean ± Standard Error through one-way analysis of variance (ANOVA). Means were separated by Tukey's B multiple range tests when ANOVA was significant ($p < 0.05$). Data statistics was performed using SPSS 25.0 software (IBM Corporation, USA).

Results and discussion

Yield and Chemical Profiling of OAEO Through GC–MS

The yield of OAEO was found to be 4 mL/kg of plant material used and chemical profiling of OAEO by GC–MS analysis revealed the presence of 27 notable components comprising 97.68% of total EO (Table 1). Results obtained through GC–MS showed citral as the major component comprising 66.72% followed by linalool (7.40%), α-bisabolene (4.65%), and isogeranial (4.65%). The percent composition of OAEO showed variation from previously reported results of Matasyoh et al. (2006) suggesting 36 notable components and 88.51% of the total EO and 43.21% of terpinen-4-ol content. Yamada et al. (2013) reported 26 components, representing 98.9% of the total EO with linalool (19.63%) and 1,8-cineole (17.27%) as major components, and Verma et al. (2016) reported camphor (41.8%) as major component whereas Sarin et al. (1992) reported citral as a major component. The notable variation in the percent composition of EO might be due to the geographical and climatic conditions, harvesting time, and methods involved during the extraction of EO (Burt, 2004). Different components present in EOs are responsible for the antifungal and anti-aflatoxigenic activity; therefore, apparent changes in the percent availability of different components could lead to a significant alteration in valuable activities of EOs (Hussain et al., 2008). Hence, the knowledge about the components and their percent composition are necessary for designing OAEO-based green preservatives for the protection of millets from fungal infestation and mycotoxin contamination.

Synthesis of OAEO Loaded Chitosan Nanoemulsion

In the present study, the synthesis of OAEO-loaded chitosan nanoemulsion (OAEO-CsNe) was performed through the ionotropic gelation method using chitosan as biopolymer and S-TPP as cross-linking agent. Previous investigation of Tavassoli-Kafrani et al. (2018) reported the encapsulation of Orange EO into gelatine nanofibers by electrospun technology and cross-linking with tannic acid. Encapsulation of cumin seed EO into active paper (synthesised by whey protein isolate and inulin) in the form of nanoemulsion by ultrasonication method has been recently reported by Hemmatkhah et al. (2020). However, in the present investigation, ionotropic gelation was used for a successful incorporation of OAEO into chitosan nanobiopolymer with effective stability. Moreover, ionotropic gelation is an unadventurous and conventional method of encapsulating EO into chitosan nanomatrix along with non-toxic nature, devoid of organic solvents, and environmental safety features (Das et al., 2021b; Hadidi et al., 2020). Chitosan was selected as polymer for encapsulation of OAEO because of its auspicious polymeric mixing property with EOs, better entrapping efficiency, biocompatibility, biodegradability, chemically reactive due to presence of 1° amine, and outstanding miscibility with other components during electrostatic interaction leading to the synthesis of small-sized nanoemulsion (Deepika et al., 2021; Zargar et al., 2015).

Loading Capacity, Encapsulation Efficiency, and Nanoparticle Yield of OAEO-CsNe

Loading capacity (LC) and encapsulation efficiency (EE) of different ratios (w/v) of chitosan to OAEO were performed for optimising maximum entrapment of OAEO into chitosan nanomatrix and the result is presented in Table 2. LC value ranged from 0.441–2.609% and EE was found in between 63.054–93.212% for 1:0.2–1:1 ratio of chitosan to OAEO (w/v). Maximum LC and EE values were recorded for the 1:0.8 ratio of chitosan to OAEO. Initially, the increment in OAEO concentration was directly proportional with an increase in LC % and EE % up to 1: 0.8 ratio, followed by decreased LC and EE values which may be due to the

attainment of saturation level. Chaudhari et al. (2020) reported EE and LC values in between 19.9–76.1 and 0.3–5.9% during the encapsulation of anethole into chitosan nanoemulsion. Tavassoli-Kafrani et al. (2018) prepared orange EO-loaded electrospun gelatin (G) and gelatin-cross-linked tannic acid (GT) nanofibers and found that encapsulation efficiency for G and GT ranged between 35–69, and 16.9–60.7%, respectively. Our result showed greater encapsulation efficiency up to 93.212% during the encapsulation of OAEO oil into chitosan nanoemulsion. The result of the present investigation is in corroboration with the findings of Hasheminejad et al. (2019) with clove EO, Das et al. (2021c) with *Anethum graveolens* EO, and Tiwari et al. (2022a) with *Cinnamomum glaucescens* EO where they found a decreased level of LC and EE after achieving a particular saturation level of chitosan to EO ratio. Additionally, the variation in LC and EE also depends on the nature and composition of the biopolymers used for the investigation. The yield of nanoparticles at maximum LC and EE values was found to be 29.781% which is in line with Hasheminejad et al. (2019) and Das et al. (2021c) having almost similar encapsulated nanoparticles yield, (28.18% and 21.47%, respectively) during encapsulation of Clove and *Anethum graveolens* EO into chitosan nanoparticle and also supported the candidature of chitosan as a polymeric material for efficient entrapment of OAEO.

Characterization of Synthesised Nanoemulsions

Determination of Morphology Through SEM

The characterisation of synthesised nanoemulsion is an important parameter to be considered prior to the assessment of its antifungal and anti-aflatoxigenic potentialities. SEM analysis of CsNe and OAEO-CsNe depicted the spherical encapsulated structures with smooth surfaces as shown in Fig. 1a and b. The size of the CsNe particles ranged between 26.20 and 108.0 nm, while in the case of OAEO-CsNe, the size of particles was found in between 46.88 and 97.75 nm. Increment in size of OAEO-CsNe nanoparticles indicated the successful loading of EO into chitosan nanomatrix. The overall decrement in particle sizes might be due to intimate bindings between chitosan, S-TPP, and OAEO, involving efficient loading and sustained release kinetics of synthesised nanoemulsion (Esmaeili & Asgari, 2015). The obtained results in the present investigation are corroborated with previous reports of Das et al. (2021d) and Deepika et al. (2021) during the encapsulation of *Pimpinella anisum*, and *Petroselinum crispum* EO, respectively into chitosan nanoparticles. Aziz and Almasi (2018) reported a mean diameter of 355 nm during the encapsulation of *Thymus vulgaris* extract into whey protein isolate films. However, the result of the present investigation showed superiority in terms of the nanometric size of OAEO-CsNe particles (< 100 nm) with greater surface-to-volume ratio, better aqueous phase solubility, delivery strategies, and stability in variable storage conditions.

Fourier Transform Infrared Spectroscopy (FTIR) Analysis

The FTIR analysis of Cs powder, CsNe, OAEO, and OAEO-CsNe are described in Fig. 1c–f) depicting the interaction between different molecular moieties. Cs powder exhibited peaks at 3450 cm^{-1} (–OH stretching), 2860 cm^{-1} (–CH stretching), 1650 cm^{-1} (–NH bending), 1382 cm^{-1} (–CH stretching), 1153 cm^{-1} (C–O stretching), 1080 cm^{-1} (–OCN and C–OCN stretching), 885 cm^{-1} (–CH stretching), and 660 cm^{-1} (–CS stretching) (Coates, 2000). In the case of CsNe, peaks 3450, 1650, 1080, and 885 cm^{-1} were shifted to 3418, 1630, 1090, and 895 cm^{-1}, respectively, and some new peaks were developed at 2915 cm^{-1} (–CH stretching), 1550 cm^{-1} (–NH bending), and 1410 cm^{-1} (–CH stretching) (Coates, 2000). OAEO showed a number of peaks at 3418 cm^{-1} (–NH stretching), 2915 cm^{-1} (–CH bending), 1667 cm^{-1} (aromatic combination bands), 1445 cm^{-1} (–CH bending), 1365 cm^{-1} (sulfonates), 1188 cm^{-1} (organic sulphates), and 833 cm^{-1} (–CH bending) (Coates, 2000). Different peaks present in OAEO indicating the presence of numerous functional groups. The presence of majority of peaks of CsNe and OAEO in OAEO-CsNe signified the successful entrapment of EO into chitosan nanoemulsion. Better interaction of OAEO components with chitosan nanobiopolymer reinforces its control delivery in the emulsion system, a prerequisite for long-term antifungal and antiaflatoxigenic effect on the stored food system.

X-Ray Diffraction (XRD) Pattern

XRD patterns of Cs powder, CsNe, and OAEO-CsNe have been shown in Fig. 2a. The Cs powder showed characteristic peak at 2θ value at 20.14° and a small shoulder peak at 10.58° indicating the crystalline and stable nature due to close packaging of constituent molecules with inter- and intramolecular hydrogen bonds. In the case of CsNe and OAEO-CsNe, reduction in height and broadening of peaks were observed, representing decrement in crystallinity and increment in amorphousness due to the destruction of inter- and intramolecular hydrogen bonds (Hosseini et al., 2013; Panda et al., 2019; Woranuch & Yoksan, 2013). Moreover, the components of nanoencapsulants were involved in cross linking of NH_3^+ group of chitosan with PO_4^{3-} group of S-TPP leading to the dissolution of crystals matrices and solvent surfaces (Amalraj et al., 2020). The alteration in diffraction patterns demonstrated inter-and intra-molecular interaction between chitosan, S-TPP, and OAEO molecules

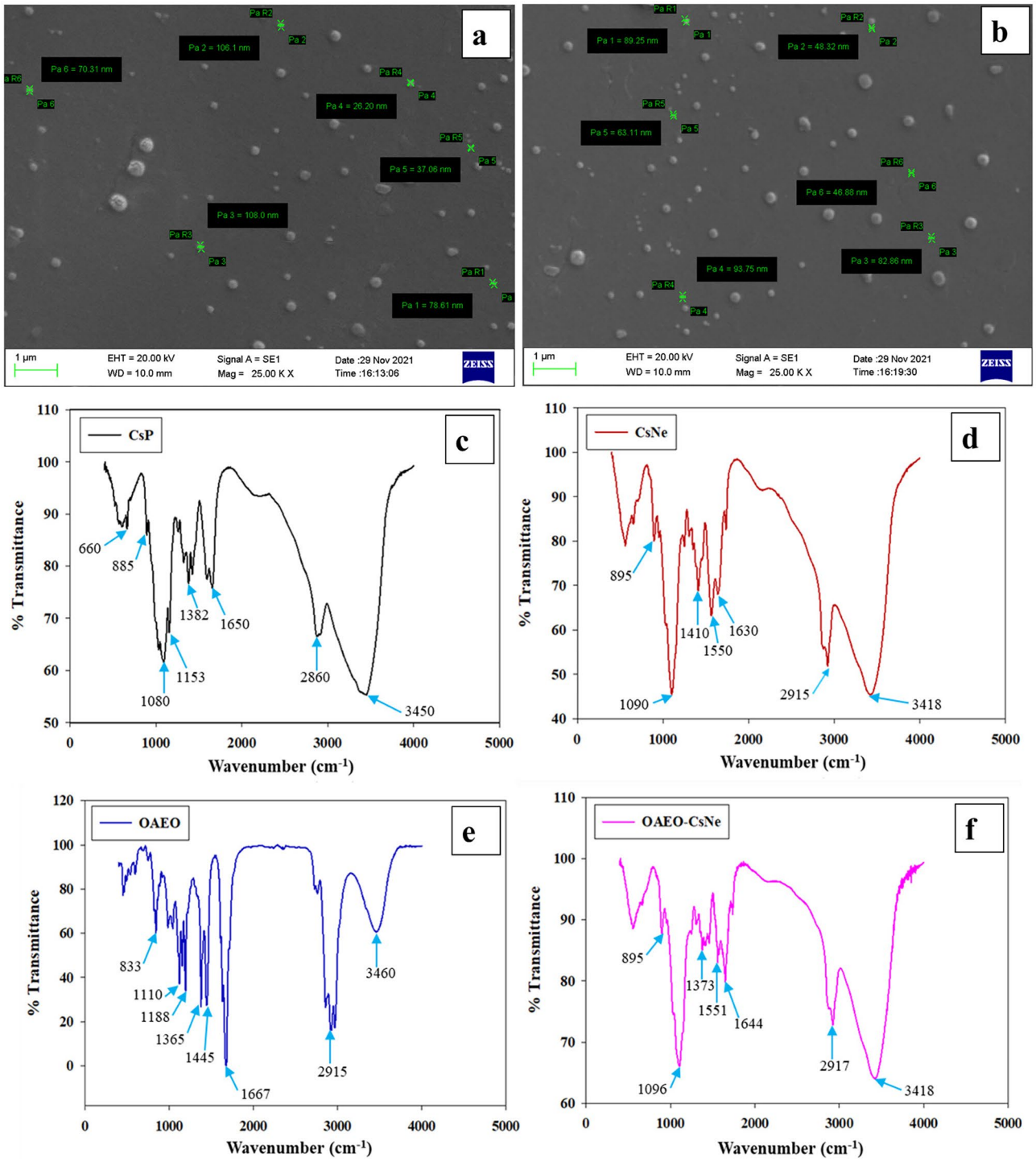

Fig. 1 Scanning electron microscopic images of CsNe and OAEO-CsNe **a** and **b**, FTIR spectra of CsP, CsNe, OAEO, and OAEO-CsNe **c**, **d**, **e**, and **f**

(Das et al., 2021d). Destruction in chitosan crystallinity after the inclusion of OAEO offers greater stability with active tight packaging of volatile components and facilitates the compatibility of OAEO-loaded chitosan nanoemulsion for practical application in the food system.

In Vitro Release Profile of OAEO-CsNe

In the present investigation, OAEO showed biphasic pattern of delivery from chitosan nanoemulsion with almost 50% burst release within 8 h followed by controlled release

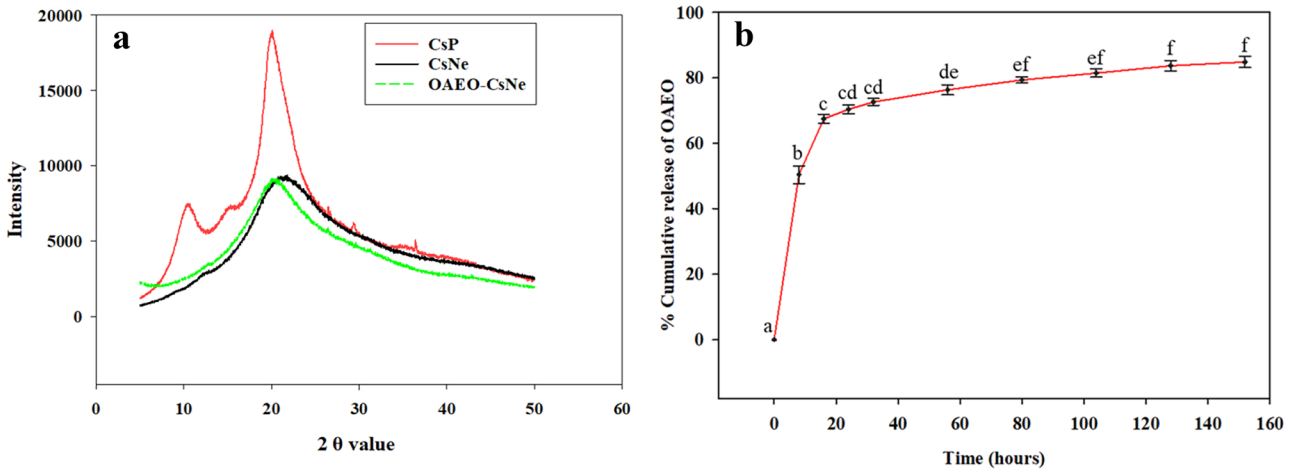

Fig. 2 X-ray diffraction patterns of CsP, CsNe, and OAEO-CsNe **a**, and in-vitro release profile of OAEO from OAEO-CsNe nanoemulsion **b**

pattern after 24 h (Fig. 2b). Initially, 84.818% OAEO was released from OAEO-CsNe, depicting that almost 8.394% of OAEO out of 93.212% still remain entrapped within chitosan nanomatrix over a period of 152 h. Our result contradicted from the previous investigation of Ghaderi-Ghahfarokhi et al. (2016) suggesting three different phases of the release of Thyme EO from chitosan nanoparticle. Surface erosion, leakage of weakly bound components, and adsorption of OAEO on the chitosan surface may be a possible reason for the initial burst release (Hariharan et al., 2008; Matshetshe et al., 2018). Similar finding on the biphasic release profile of tannic acid from sugarcane bagasse packaging films has been recently observed (Lee et al., 2020). They suggested initial burst release of tannic acid in the first 30 min followed by later sustained release within 2–6 h. De Souza et al. (2018) demonstrated the higher release (42–54%) of *Citrus aurantium* EO from polymeric formulation containing maltodextrin, gum arabic, and cellulose nanofibrils within very short periods of time (0–150 min). This is the first-time report on controlled and sustained delivery of OAEO from chitosan nanoemulsion up to a period of 152 h, a prerequisite for gradual antifungal effect on the food system. Controlled release of OAEO is very useful in maintaining long-term effect, masking intense aroma of EO, and in prevention of organoleptic properties without being in contact with food commodities (da Silva et al., 2018). The result obtained in the present investigation is in line with the previous investigation of Tiwari et al. (2022b) suggesting a biphasic release profile of *Homalomena aromatica* EO from chitosan nanomatrix. Obtained results signified strong candidature of OAEO-CsNe as smart protectant against fungal infestation, AFB_1 secretion, and oxidative damage in stored food commodities.

In Vitro Antifungal and AFB_1 Inhibitory Efficacy of OAEO and OAEO-CsNe

The in vitro antifungal and anti-aflatoxigenic activities of OAEO and OAEO-CsNe were assessed for the first time at different concentrations and results are represented in terms of MIC and MAIC of AFLHPSi-1 cells in Table 3. MIC and MAIC of OAEO were found to be 0.400 and 0.350 µL/mL, respectively, while in the case of OAEO-CsNe, enhancement in antifungal and antiaflatoxigenic activity were recorded with MIC and MAIC values 0.200 and 0.175 µL/mL, respectively. In a study conducted by Kujur et al. (2021), the antifungal and AFB_1 inhibitory concentration in *A. flavus* were found to be 3.0 and 2.5 µL/mL for nanoencapsulated Jasmine EO. The MIC and MAIC values of nanoencapsulated *C. glaucescens* EO against *A. flavus* were found to be 0.9 and 0.8 µL/mL, respectively (Tiwari et al., 2022a). Previous investigation of Fabra et al. (2016) reported effective inhibition of pathogenic fungi such as *Rhizopus stolonifer* and *Alternaria* sp. by carvacrol incorporated into chitosan and zein nanocapsules. However, our result showed almost three to seven-fold better bioefficacy for inhibition of *A. flavus* growth and AFB_1 production. Enhancement in antifungal activity of OAEO-chitosan nanostructured emulsion has been attributed by efficient encapsulation and availability of active components of EO, slowdown degradation, controlled release for longer time, and specific delivery of nanostructured emulsion to the plasma membrane of target organism (Das et al., 2021a). The reduction in fungal sporulation, inhibition of enzymes responsible for carbohydrate catabolism, and downregulation of key enzymes involved in the biosynthesis of AFB_1 might be responsible for reduced AFB_1 production (López-Meneses et al., 2018). Our results

agreed with some of the investigations conducted by, Roshan et al. (2021, 2022) with *Pogostemon cablin* (Blanco) Benth. EO and *Toddalia asiatica* (L.) Lam. EO. The application of OAEO-loaded chitosan nanoemulsion having enhanced bioefficacy could be an effective strategy for the preservation of stored food commodities against the fungal proliferation and AFB_1 contamination instead of widely used harmful synthetic preservatives.

Antifungal and Antiaflatoxigenic Mode of Action

Effect of OAEO and OAEO-CsNe on Membrane Ergosterol

Ergosterol is predominant sterol component found in the fungal cell membrane and involved in the maintenance of cell integrity, function, and also act as one of the major sites for most of the antifungal drugs. Its biosynthesis is a complex process involving multiple enzymes, hence, the loss of any enzyme led to a disparity in cell membrane permeability and functioning (Cai et al., 2019). Percent reductions of ergosterol level in OAEO fumigated AFLHPSi-1 cells were found to be 12.11%, 30.60%, 40.11%, 57.83%, 64.87%, 82.47%, 92.54%, and 100% for 0.050, 0.100, 0.150, 0.200, 0.250, 0.300, 0.350, and 0.400 µL/mL, respectively. However, OAEO-CsNe caused enhanced efficacy for the inhibition of ergosterol biosynthesis (Table 4). Superior efficacy of OAEO-CsNe for ergosterol inhibition at lower doses might be due to synergism between chitosan and OAEO in the nanoemulsion system with smaller size and better penetrability in target organisms' membrane facilitating greater diffusion of active components (Das et al., 2021b; Xu et al., 2021).

Cellular ions and 260/280 Absorbing Materials Leakage

In the present investigation, a considerable increase in the release of vital cellular ions (Ca^{2+}, Mg^{2+}, and K^+) and 260, 280 nm absorbing materials from OAEO and OAEO-CsNe treated AFLHPSi-1 cells were recorded for the first time which directly indicated plasma membrane as the primary site for antifungal action (Fig. 3 a–d). Previous investigation of Kujur et al. (2021) demonstrated leakage of Mg^{2+} (6.0–8.0 mg/L), Ca^{2+} (10–12 mg/L), and K^+ (200–300 mg/L) ions from toxigenic *A. flavus* cells after fumigation with nanoencapsulated jasmine EO; however, our result showed excessive leakage of Ca^{2+} (30–60 mg/L) and Mg^{2+} (20–60 mg/L) ions in the extra cellular media after fumigation with different doses of OAEO-CsNe, suggesting extreme damage of plasma membrane integrity and permeability. The membrane damage resulted into the dismantling of cellular respiratory system and vital functions of organelles such as peroxisomes, endosomes, Golgi body, endosomal vacuoles, and endoplasmic reticulum leading to deleterious effect on AFB_1 biosynthesis (Das et al., 2021d). The OAEO-CsNe showed increased leakage of vital cellular components of AFLHPSi-1 cells because of nano-sized particles which empower it to pass quickly through the plasma membrane causing greater damage to fungal cells. Cellular ions play important role in hyphal growth, homeostasis maintenance, protein synthesis, and ATP generation in fungal cells (Udeh & Kgatla, 2013). Moreover, 260 and 280 nm absorbing materials provide an idea about the extent of nucleic acid and protein leakage from OAEO and OAEO-CsNe-treated fungal cells. The nucleic acids and proteins are chief components responsible for maintaining the physiological functions of fungal cells (Deepika et al., 2021). From the obtained results, it has been proposed that impairment in plasma membrane fluidity and permeability after OAEO and OAEO-CsNe treatment led to effective inhibition of fungal growth.

Cellular Methylglyoxal (MG) Determination

Figure 3e, f indicates a dose-dependent decrease in MG level after fumigation of AFLHPSi-1 cells with OAEO and OAEO-CsNe. Control sets showed the highest MG level (462.76 and 473.09 µM/g FW), whereas the level of MG in AFLHPSi-1 cells fumigated with OAEO at 0.050, 0.100, 0.150, 0.200, 0.250, 0.300, 0.350, and 0.400 µL/mL was found to be 462.76, 433.33, 388.10, 346.39, 340.15, 288.49, 227.48, and 181.67 µM/g FW, respectively. OAEO-CsNe exhibited better efficacy for inhibition of MG biosynthesis in AFLHPSi-1 cells as 473.09, 420.27, 371.34, 335.86, 312.67, 267.64, 208.77, 173.48, and 128.26 µM/g FW at 0.025, 0.050, 0.075, 0.100, 0.125, 0.150, 0.175, and 0.200 µL/mL, respectively. MG acts as aflatoxin inducer in *A. flavus* cells by upregulating the expression of *afl-R* and *ver-1* genes, involved in aflatoxin biosynthesis regulation (Chen et al., 2004; Chaudhari et al., 2022). Therefore, a decrease in cellular level of MG could be correlated with the reduction in AFB_1 biosynthesis. Das et al. (2021c) reported inhibition of methylglyoxal biosynthesis in *A. flavus* (AF LHP R14) cells upto a level of 433.99 µM/gFW after fumigation with nanoencapsulated *Anethum graveolens* EO. However, in the present study, OAEO-CsNe was found to inhibit the MG level in treated AFLHPSi-1 cells more effectively than unencapsulated OAEO, hence, causing greater suppression of gene upregulation required for AFB_1 biosynthesis. Our result is in line with investigations conducted by Deepika et al. (2021) for a reduction in methylglyoxal biosynthesis in *A. flavus* cells after fumigation with nanoencapsulated *Petroselinum crispum* EO.

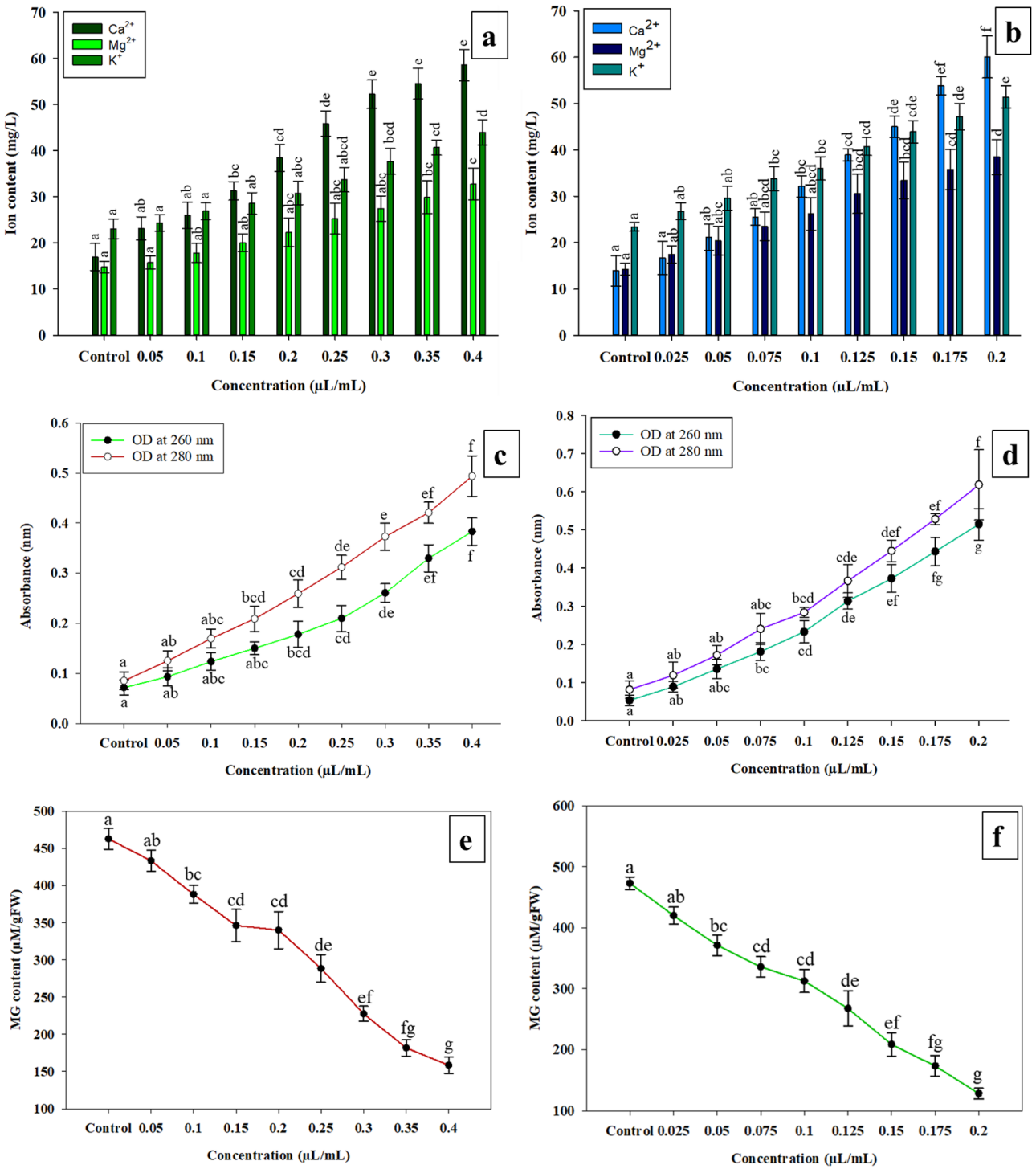

Fig. 3 Effect of different concentrations of OAEO **a** and OAEO-CsNe **b** on cellular ions leakage **a** and **b**, effect of different concentration of OAEO **c** and OAEO-CsNe **d** on 260 and 280 nm absorbing materials leakage, and effect of on cellular methylglyoxal level of AFLHPSi-1 cells **e** and **f**

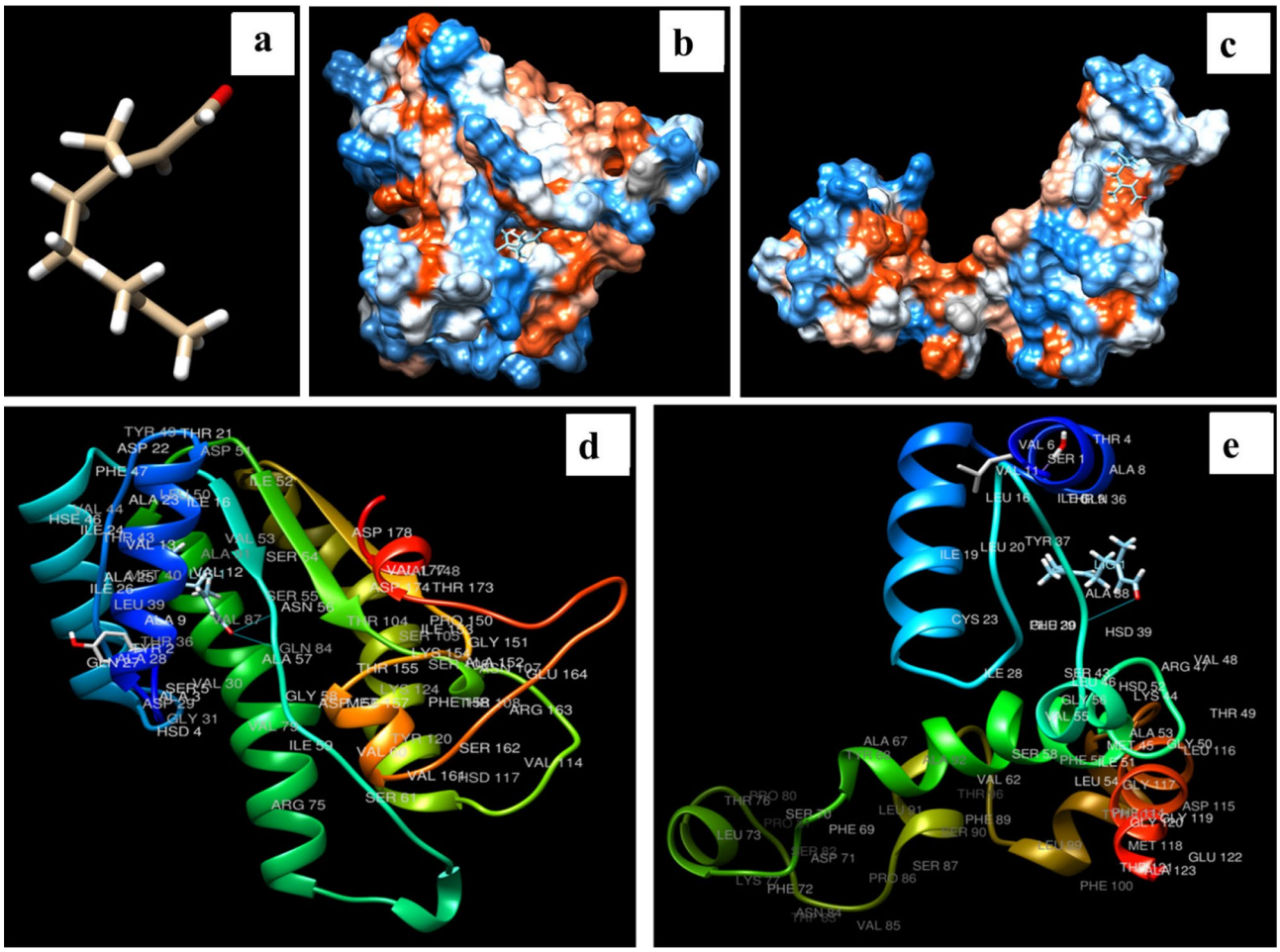

Fig. 4 3-D structure of citral **a**, Ver-1 and Omt-A protein structures **b** and **c**, interaction of citral with ASN-56, ALA-57, and HSD-39 amino acids in Ver-1 and Omt-A proteins **d** and **e**

In Silico Molecular Modelling of Citral with Ver-1 and Omt-A Proteins

The molecular mechanism of AFB_1 inhibition was examined through in silico docking of citral (major component of OAEO) with Ver-1 and Omt-A proteins. Ver-1 and Omt-A proteins are involved in the conversion of versicolorin to sterigmatocystin and sterigmatocystin to dihydro-*o*-methylsterigmatocystin in AFB_1 biosynthesis pathways (Singh et al., 2020; Xing et al., 2017). The docking between the 3D-structure of citral (downloaded from PubChem database) and Ver-1 and Omt-A proteins (obtained from Phyre 2 online server by uploading FASTA sequence) was performed by UCSF Chimera software (Fig. 4a–c). Citral was effectively interacted with ASN-56 and ALA-57 amino acids of Ver-1 via hydrogen bonding with binding energy – 5.981 kcal/mol and HSD-39 amino acid of Omt-A protein with binding energy – 5.920 kcal/mol (Table 5 and Fig. 4d, e). Kujur et al. (2021) demonstrated the molecular interaction of benzyl acetate, α-hexylcinnamaldehyde, and α-pinene (major components of jasmine EO) with Ver-1 and Omt-A proteins of AFB_1 biosynthesis by hydrogen bonding having the binding energy in between – 4.87 to – 36.71 kcal/mol. Contrary to the study of Kujur et al. (2021), our result suggested better interaction of citral against Ver-1 and Omt-A proteins by more hydrogen bonds with binding energy – 5.981 and – 5.920 kcal/mol. The hydrogen bond interaction of citral might mediate the structural variation of Ver-1 and Omt-A proteins leading to the inhibition of AFB_1 biosynthesis. The lower binding energy indicated the strong binding affinity of citral with Ver-1 and Omt-A proteins (Singh et al., 2015). Our study is corroborated with a similar study conducted by Prasad et al. (2022) in which citral interacted with GLY 18 and ALA 41 amino acids of Ver-1 protein and ARG 47 amino acid of Omt-A proteins with efficient inhibition of AFB_1 biosynthesis.

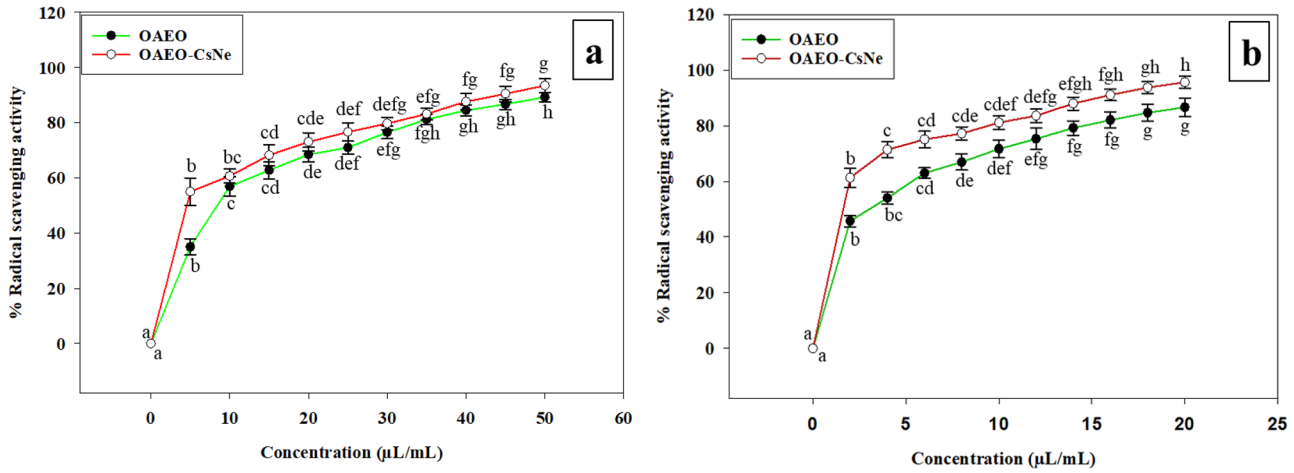

Fig. 5 Antioxidant activity of OAEO and OAEO-CsNe by DPPH **a** and ABTS **b** assay

Total Phenolic Content and Antioxidant Activity of OAEO and OAEO-CsNe

Total phenolic content of OAEO was found to be 5.116 µg gallic acid equivalent and nanoencapsulated OAEO depicted enhancement in the phenolic content as 7.149 µg gallic acid equivalent. The antioxidant activity of OAEO and OAEO-CsNe were determined through $DPPH^{\bullet+}$ and $ABTS^{\bullet+}$ assay and expressed in terms of IC_{50} (concentration at which 50% scavenging of free radicals occurs) values. The antioxidant activity of OAEO was mainly due to components such as citral, linalool, and isogeranial (Ahmadi et al., 2021). The IC_{50} value of OAEO was found to be 8.360 and 3.105 µL/mL through $DPPH^{\bullet+}$ and $ABTS^{\bullet+}$ assay, respectively. However, OAEO-CsNe displayed better antioxidant activities with IC_{50} values of 4.542 µL/mL and 1.647 µL/mL through $DPPH^{\bullet+}$ and $ABTS^{\bullet+}$ assay, respectively (Fig. 5). Improvement in antioxidant activity of *Thymus vulgaris* extract incorporated into whey protein isolate nanoliposomes has been recently demonstrated by Aziz and Almasi (2018). Significant hydrogen bonding interaction of hydroxyl groups of phenolic components with polycationic wall matrix causing the sustainable release of the extract could be suggested as a possible mechanism for enhancement in antioxidant activity. Previous investigation of Danh et al. (2013) suggested 63% neutralisation of DPPH molecules by *Lavandula angustifolia* EO at maximum dose. However, our results showed superiority for 100% neutralisation of DPPH and ABTS molecules as compared to abovementioned investigations at very low doses of OAEO. More importantly, the OAEO after encapsulation into chitosan nanoemulsion enhanced the free radical scavenging potentiality, and 100% neutralisation was achieved at very low concentration as compared to unencapsulated OAEO. Improved antioxidant activity of OAEO-CsNe as compared to unencapsulated OAEO might be due to better solubility of small-sized nanoemulsion containing EO in medium with controlled delivery and greater scavenging of free radicals generated in the medium. Enhanced free radical scavenging activity after encapsulating clove EO in chitosan matrix has been reported by Hadidi et al. (2020). Moreover, fungal infestation and AFB_1 contamination induce the ROS production leading to lipid peroxidation-mediated biodeterioration of stored food commodities. Hence, OAEO-CsNe with better phenolic content and enhanced free radical scavenging activity could be used for the preservation of stored millets and other agricultural food commodities to mitigate oxidative deterioration.

In Situ Efficacy of OAEO and OAEO-CsNe: HPLC Analysis in *S. italica* Seeds

OAEO and OAEO-CsNe demonstrated significant in vitro antifungal and AFB_1 inhibitory activity, as well as potential biochemical mechanisms of action, although, these findings may not necessarily translate to actual efficacy in a real food system. As a result, the in situ effectiveness of OAEO and OAEO-CsNe was evaluated in *S. italica* seeds as a model millet food system for 1 year of storage. Control samples had the highest AFB_1 level (14.00 µg/kg), the AFB_1 content in *S. italica* seeds fumigated with MIC dose of OAEO was found to be 0.445 µg/kg whereas at 2MIC dose of OAEO there was complete inhibition of AFB_1 content was recorded. Hundred percent inhibition of AFB_1 biosynthesis in *S. italica* seeds was also recorded for OAEO-CsNe for MIC and 2MIC doses. Due to the absorption/adsorption of OAEO components at some extent by the stored food item itself, a greater dose of OAEO was required for complete suppression of AFB_1 in *S. italica* seeds in the present investigation. The nanorange size, greater shelf-life of particles, and regulated

release of OAEO-CsNe over a longer period of time are responsible for better AFB_1 inhibition in the model millet food system (Das et al., 2021b; Pabast et al., 2018). Our result corroborated with the previous finding of Buendía-Moreno et al. (2019) suggesting cinnamon, carvacrol, and oregano-based nanoparticle encapsulated into β-cyclodextrin nanocomposite for postharvest preservation of tomatoes against microbial infestation. They described the bacteriostatic and fungitoxic activity up to 29–36% by β-cyclodextrin loaded cinnamon, carvacrol, and oregano nanocomposite over a period of 22 days. Tiwari et al. (2022a) tested the efficacy of *C. glaucescens* EO in stored *Nigella sativa* seeds, and reported that AFB_1 content was reduced up to 9.3 µg/kg after 1.5 year of storage periods. Contrary to the above-mentioned investigations, our result suggested complete inhibition of fungal infestation and AFB_1 biosynthesis (100%) at MIC and 2 MIC doses of OAEO-CsNe. Moreover, OAEO-CsNe showed excellent antifungal and antiaflatoxigenic activity for preservation of millet food system as compared to commonly used organic preservatives like propionic acid, formic acid, acetic acid, and benzoic acid (Dwivedy et al., 2018). This is the first time report on in situ preservative potentialities of nanoencapsulated OAEO in stored millet seeds with emphasis on antiaflatoxigenic activity. The findings of this study showed that nanoencapsulated OAEO could be used as a next-generation green preservative to prevent AFB_1-mediated biodeterioration of stored millets and other agricultural commodities in place of harmful effects of synthetic preservatives.

Effect of OAEO and OAEO-CsNe on Lipid Peroxidation Estimation

Lipid peroxidation in stored food commodities causes degradation of nutritional components, off-flavour, undesirable changes in organoleptic properties, off-taste, and decreased shelf-life. Chemical preservatives such as BHT

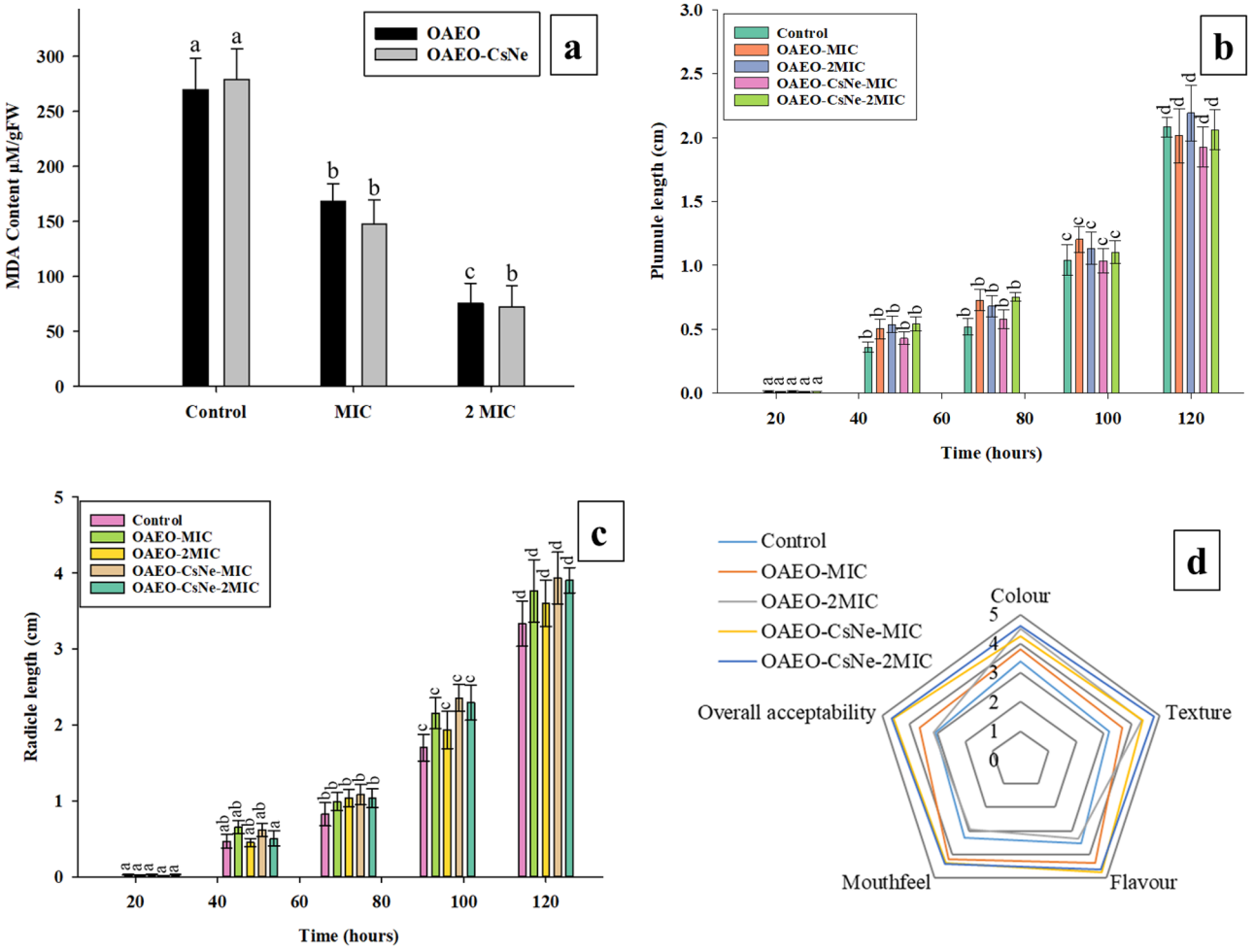

Fig. 6 Effect of OAEO and OAEO-CsNe on of lipid peroxidation **a**, phytotoxicity **b** and **c**, and sensory profile **d** of *S. italica* seed samples treated with OAEO and OAEO-CsNe at MIC and 2MIC doses

Table 1 Chemical profiling of OAEO through GC–MS

S. no	Components	RT (min)	Percent composition	RI (Adams, 2007)	RI (calculated)
1	Sulcatone	8.49	2.84	-	970
2	Limonene	10.098	0.28	1024	1012
3	β-Ocimene	10.905	0.65	1032	1031
4	Linalool	13.436	7.40	1095	1092
5	(E)-Salvene	14.851	0.37	858	1121
6	Citronellal	15.590	0.28	1148	1135
7	Isogeranial	16.472	4.65	-	1147
8	Piperitone	20.458	0.33	1250	1246
9	**Citral**	**20.876**	**66.72**	**1316**	**1259**
10	Epoxy-linalool oxide	21.820	0.86	-	1273
11	Neryl acetate	24.819	0.33	1359	1344
12	Geranyl acetate	25.656	0.30	1379	1364
13	cis-3-Hexenyl lactate	25.884	0.30	1197	1368
14	β-Caryophyllene	27.049	1.77	1417	1395
15	α-Bergamotene	27.709	1.31	1432	1411
16	Humulene	28.498	0.71	1436	1430
17	β-Famesene	28.628	0.37	-	1435
18	Germacrene-D	29.564	0.78	1508	1456
19	β-Bergamotene	29.730	0.20	1432	1461
20	γ-Bisabolene	30.773	0.23	1529	1486
21	α-Bisabolene	32.163	4.65	1506	1522
22	Caryophyllene oxide	33.506	0.52	1582	1556
23	Humulene oxide	34.571	0.22	1608	1600
24	α-Bisabolol	37.603	0.23	1601	1658
25	Nerolidyl acetate	50.053	0.44	1676	2030
26	α-Cedrene	51.268	0.47	1410	2072
27	Linoleic acid	52.323	0.47	2133	2104
	Total		**97.68**		

Major component in bold

-=not determined

(butylated hydroxytoluene) are commonly used to minimise the peroxidation effect, but it is associated with a debate for causing cancer, behavioural risks, and asthma (EFSA, 2012; Błaszczyk et al., 2013). Hence, EOs and its nanoemulsion could be a promising candidate for inhibition of lipid peroxidation in stored millet system with greater

Table 2 Encapsulation efficiency, loading capacity, and yield of OAEO-CsNe nanoparticles

Chitosan: OAEO (w/v)	% Encapsulation efficiency	% Loading capacity	Nanoparticle's yield (%)
1:0	0.000 ± 0.000^{a}	0.000 ± 0.000^{a}	-
1:0.2	63.054 ± 4.416^{b}	0.441 ± 0.030^{b}	-
1:0.4	74.654 ± 6.194^{bc}	1.045 ± 0.087^{c}	-
1:0.6	83.372 ± 4.409^{bc}	1.750 ± 0.092^{d}	-
1:0.8	$\mathbf{93.212 \pm 2.531^{cd}}$	$\mathbf{2.609 \pm 0.070^{e}}$	$\mathbf{29.781 \pm 1.753}$
1:1	73.204 ± 3.304^{d}	2.562 ± 0.115^{e}	-

Values are mean ($n=3$) ± standard error

The bolded values represents the ratio suggesting maximum encapsulation efficiency, loading capacity, and nanoparticle yield

Different letters in superscript represent significant differences at p value <0.05 according to ANOVA and Tukey's B multiple range test

-=not determined

shelf-life and better antioxidant potentiality. Peroxidation of polyunsaturated fatty acids resulted into the production of malondialdehyde (MDA). In the present study, OAEO and OAEO-CsNe maintained the lower level of MDA in *S. italica* seeds at MIC (168.43 and 147.61 µM/gFW) and at 2MIC (75.52 and 72.25 µM/gFW) doses as compared to control sets (269.76 and 279.22 µM/gFW) (Fig. 6a). Souza et al. (2015) evaluated the effect of nano-multilayered coating of sodium alginate and chitosan matrix prepared through polyelectrolyte complexes on fresh cut mango for effective reduction of MDA level (8–10 µM/g FW) by inhibiting the senescence dependent lipid peroxidation up to 8 days of storage. Encapsulation of Thyme EO into sodium alginate caused a significant decrement of MDA content (200–600 µmol/g FW) in postharvest *Pholiota nameko* mushroom by improving the antioxidant activities has been recently reported (Zhu et al., 2019). However, our result demonstrated greater efficacy of OAEO-CsNe for inhibition of lipid peroxidation in the millet food system which has been associated with greater antioxidant activity, and controlled release of active components (Navikaite-Snipaitiene et al., 2018), resulting into improvement in millet shelf-life over a period of one year and maximise its efficacy as a novel plant-based shelf-life enhancer in food and agricultural industries.

Safety Profile Assessment of OAEO and OAEO-CsNe

Safety assessment of OAEO and OAEO-CsNe was evaluated on mice and LD_{50} values were recorded as 7798.4 and 11,162.06 µL/kg, respectively. The LD_{50} of nanoencapsulated OAEO was found much higher than the unencapsulated form. Some of the organophosphate fungitoxicants such as parathion and tetraethyl-pyrophosphate showed very low LD_{50} (1–25 mg/kg) on mammalian systems while LD_{50} of botanical preservatives such as azadirachtin and pyrethrum were 5000 and 350–500 mg/kg. However, LD_{50} of OAEO and OAEO-CsNe was found much higher than the recommended cut-off (5000 mg/kg) set by Organisation for Economic Co-operation and Development (OECD) (Coats, 1994; Isman, 2006) which supports its strong candidature for utilisation as a safe green preservative in food and agricultural industries. However, before the recommendation of OAEO-CsNe large-scale industrial trials should be conducted for additional safety measurements.

Phytotoxicity Evaluation of OAEO and OAEO-CsNe

The *S. italica* seeds fumigated with OAEO and OAEO-CsNe exhibited good germination (emergence of plumule and radicle) within 4–5 days which is similar to the control seeds and did not show any negative effect

Table 3 Effect of OAEO and OAEO-CsNe on mycelial weight and aflatoxin B_1 production by AFLHPSi-1

Concentration (µL/mL)	OAEO				Concentration (µL/mL)	OAEO-CsNe			
	Mycelial weight (g)	% Reduction of fresh weight	AFB_1 (µg/L)	% AFB_1 reduction		Mycelial weight (g)	% Reduction of fresh weight	AFB_1 (µg/L)	% AFB_1 reduction
Control	0.348 ± 0.020^{a}	0.000 ± 0.000^{a}	5214.312 ± 378.327^{a}	0.000 ± 0.000^{a}	Control	0.338 ± 0.018^{a}	0.000 ± 0.000^{a}	4761.101 ± 290.304^{a}	0.000 ± 0.000^{a}
0.050	0.297 ± 0.015^{ab}	14.509 ± 3.904^{ab}	3721.101 ± 415.374^{b}	29.072 ± 3.013^{b}	0.025	0.294 ± 0.024^{b}	13.407 ± 3.636^{b}	3558.899 ± 219.293^{b}	24.886 ± 5.334^{b}
0.100	0.245 ± 0.015^{bc}	29.763 ± 0.939^{bc}	2256.514 ± 252.979^{c}	55.475 ± 8.699^{c}	0.05	0.238 ± 0.023^{c}	28.995 ± 8.804^{c}	2342.385 ± 209.256^{c}	50.616 ± 4.545^{c}
0.150	0.204 ± 0.010^{c}	40.777 ± 6.147^{c}	$1645.872 \pm 244.562^{cd}$	67.354 ± 7.558^{cd}	0.075	0.190 ± 0.010^{d}	43.669 ± 1.166^{d}	1927.339 ± 164.085^{c}	59.411 ± 3.255^{c}
0.200	0.127 ± 0.024^{d}	62.603 ± 8.538^{d}	$1226.055 \pm 204.804^{de}$	75.600 ± 6.109^{de}	0.100	0.157 ± 0.018^{d}	53.649 ± 4.333^{e}	1106.789 ± 101.984^{d}	76.784 ± 1.300^{d}
0.250	0.048 ± 0.012^{e}	88.258 ± 3.759^{e}	529.541 ± 103.204^{ef}	89.780 ± 1.879^{ef}	0.125	0.073 ± 0.011^{d}	78.528 ± 2.681^{e}	586.789 ± 144.779^{de}	87.739 ± 2.990^{de}
0.300	0.018 ± 0.002^{e}	94.632 ± 1.099^{e}	190.825 ± 58.622^{f}	96.307 ± 1.072^{f}	0.150	0.028 ± 0.008^{d}	91.841 ± 1.864^{e}	209.908 ± 66.275^{e}	95.610 ± 1.407^{e}
0.350	0.008 ± 0.002^{e}	97.629 ± 0.689^{e}	0.000 ± 0.000^{f}	100.000 ± 0.000^{f}	0.175	0.013 ± 0.003^{d}	96.224 ± 0.684^{e}	000.000 ± 0.000^{e}	100.000 ± 0.000^{e}
0.400	0.000 ± 0.000^{e}	100.000 ± 0.000^{f}	0.000 ± 0.000^{f}	100.000 ± 0.000^{f}	0.200	0.000 ± 0.000^{f}	100.000 ± 0.000^{e}	0.000 ± 0.000^{e}	100.000 ± 0.000^{e}

AFB_1 = aflatoxin B_1

Values are mean ($n = 3$) ± standard error

Different letters in superscript represent significant differences at p value <0.05 according to ANOVA and Tukey's B multiple range test

Table 4 Effect of OAEO and OAEO-CsNe on ergosterol reduction in AFLHPSi-1 cells

Concentration (µL/mL)	OAEO		Concentration (µL/mL)	OAEO-CsNe	
	Mycelial fresh weight (g)	% Reduction of ergosterol		Mycelial fresh weight (g)	% Reduction of ergosterol
Control	1.035 ± 0.039^{a}	0.000 ± 0.000^{a}	Control	0.962 ± 0.002^{a}	0.000 ± 0.000^{a}
0.05	0.954 ± 0.005^{b}	12.110 ± 5.245^{a}	0.025	0.938 ± 0.003^{b}	6.794 ± 2.630^{b}
0.1	0.847 ± 0.005^{c}	30.609 ± 4.331^{b}	0.05	0.820 ± 0.011^{c}	32.282 ± 2.887^{c}
0.15	0.749 ± 0.007^{d}	40.118 ± 6.136^{b}	0.075	0.731 ± 0.010^{d}	53.180 ± 1.062^{d}
0.2	0.520 ± 0.002^{e}	57.832 ± 2.102^{c}	0.1	0.482 ± 0.005^{e}	65.506 ± 1.011^{e}
0.25	0.329 ± 0.007^{f}	64.879 ± 3.326^{c}	0.125	0.303 ± 0.004^{f}	75.374 ± 1.521^{f}
0.3	0.242 ± 0.023^{g}	82.479 ± 3.135^{d}	0.15	0.217 ± 0.008^{g}	88.507 ± 1.110^{g}
0.35	0.176 ± 0.002^{h}	92.548 ± 0.763^{de}	0.175	0.163 ± 0.003^{h}	95.506 ± 0.807^{h}
0.4	0.000 ± 0.000^{i}	100.000 ± 0.000^{e}	0.2	0.000 ± 0.000^{h}	100.000 ± 0.000^{h}

Values are mean ($n = 3$) ± standard error

Different letters in superscript represent significant differences at p value <0.05 according to ANOVA and Tukey's B multiple range test

(Fig. 6b, c). Alipour et al. (2019) in a study demonstrated the significant reduction in seed germination of radish and amaranth when treated with encapsulated rosemary Peretto et al. (2017) also reported the phytotoxic effect of EO-loaded chitosan coating on strawberry fruits. However, our results contradicted with the abovementioned investigations and found non-toxic nature of both OAEO and OAEO-CsNe on model millet system supporting its application as natural green fumigants for stored food commodities which can be utilised for sowing purposes in upcoming seasons.

Sensorial Properties Evaluation of Fumigated Stored Model Food Commodity

The sensory analysis of stored *S. italica* seeds (model food commodity) before and after fumigation with OAEO and OAEO-CsNe is a necessary parameter prior to presenting consumers for acceptance. Fumigated seeds exhibited satisfactory acceptance in terms of the colour, texture, flavour, mouth feel, and overall acceptability at MIC and 2MIC doses of OAEO and OAEO-CsNe (Fig. 6d). There were slight improvements in sensorial parameters were observed at MIC doses of OAEO, while at 2MIC doses, greater improvement was observed for texture and colour of seeds. However, at 2MIC dose of OAEO fumigation, less scores were obtained for flavour, mouth feel, and overall acceptability, which has been associated with a higher dose of EO and its persistent intense aroma in seeds. An investigation of Lai et al. (2013) demonstrated that Cinnamon EO-loaded tapioca starch/hsian-tsao leaf gum nanoparticle could maintain the acceptable organoleptic properties of fresh cut carrots over a period of 16 days. However, in our investigation, better scores were obtained for all the sensory parameters after fumigation with MIC and 2MIC doses of nanoencapsulated OAEO without any negative impacts on the stored food system. Our result is in line with the previous investigation of Tiwari et al. (2022a) suggesting maintenance of sensory parameters after fumigating *N. sativa* seeds with *C. glaucescens* EO and its nanoencapsulated formulations. This is the first report on the maintenance of sensorial properties in stored *S. italica* seeds after fumigation with nanoencapsulated OAEO and maximise its efficacy for utilisation in future consumption purposes.

Table 5 Binding energy of OAEO (citral molecule) with Ver-1 and Omt-A proteins

Major component of OAEO	Receptor protein	H-bonding amino acid	Binding energy (Kcal/mol)	Bond length(Å)
Citral	Ver-1	ASN-56 ALA-57	−5.981	2.472 2.010
	Omt A	HSD-39	−5.920	2.622

Conclusion

Encapsulated OAEO (OAEO-CsNe) depicted enhanced efficacy against fungal growth, AFB_1 secretion, and lipid peroxidation in stored millet system. Antifungal mechanism of action of OAEO-CsNe was associated with the inhibition of ergosterol biosynthesis, and leakage of vital cellular constituents. Inhibition of methylglyoxal biosynthesis suggested as the mechanism of AFB_1 inhibition. In silico molecular docking confirmed the molecular interaction of citral with Ver-1 and Omt A proteins resulting into the inhibition of AFB_1 biosynthesis. The fruitful in situ efficacy in the protection of stored *S. italica* seed samples from AFB_1 contamination, lipid peroxidation, non-phytotoxic behaviour, satisfactory safety profile, and acceptable sensory evaluation strengthens the possibilities for application of OAEO-CsNe as a potential green preservative in food and agricultural industries.

Acknowledgements Bijendra Kumar Singh is grateful to Head, Department of Botany, and Principal of Feroze Gandhi College, Raebareli, Uttar Pradesh, India for kind support. Authors are thankful to Head and Coordinator, CAS, Department of Botany, ISLS, for providing laboratory facilities, and Central Instrument Facility, Indian Institute of Technology, Banaras Hindu University, Varanasi for SEM, FTIR and XRD analysis.

Author Contribution Bijendra Kumar Singh: conceptualization, methodology, writing original draft, data curation, and funding acquisition. Shikha Tiwari: data curation. Akash Maurya: data curation. Somenath Das: review and editing. Vipin Kumar Singh: review and editing. Nawal Kishore Dubey: supervision and writing—review and editing.

Funding Bijendra Kumar Singh is thankful to the Council of Scientific and Industrial Research (CSIR) (grant no.: 09/013(0920)/2019-EMR-I), New Delhi, India for providing research fellowship.

Data Availability The authors confirm that the data supporting the findings of this study are available within the article.

Declarations

Conflict of Interest The authors declare no competing interests.

References

Adams, R. P. (2007). *Identification of essential oil components by gas chromatography/mass spectrometry* (Vol. 456). Allured publishing corporation.

Ahmadi, T., Shabani, L., & Sabzalian, M. R. (2021). LED light sources improved the essential oil components and antioxidant activity of two genotypes of lemon balm (Melissa officinalis L.). *Botanical Studies*, *62*(1), 1–13. https://doi.org/10.1186/s40529-021-00316-7

Ali, A., Yeoh, W. K., Forney, C., & Siddiqui, M. W. (2018). Advances in postharvest technologies to extend the storage life of minimally processed fruits and vegetables. *Critical Reviews in Food Science and Nutrition, 58*(15), 2632–2649. https://doi.org/10.1080/10408398.2017.1339180

Alipour, M., Saharkhiz, M. J., Niakousari, M., & Damyeh, M. S. (2019). Phytotoxicity of encapsulated essential oil of rosemary on germination and morphophysiological features of amaranth and radish seedlings. *Scientia Horticulturae, 243*, 131–139. https://doi.org/10.1016/j.scienta.2018.08.023

Alshannaq, A., & Yu, J. H. (2017). Occurrence, toxicity, and analysis of major mycotoxins in food. *International Journal of Environmental Research and Public Health, 14*(6), 632. https://doi.org/10.3390/ijerph14060632

Amalraj, A., Haponiuk, J. T., Thomas, S., & Gopi, S. (2020). Preparation, characterization and antimicrobial activity of polyvinyl alcohol/gum arabic/chitosan composite films incorporated with black pepper essential oil and ginger essential oil. *International Journal of Biological Macromolecules, 151*, 366–375. https://doi.org/10.1016/j.ijbiomac.2020.02.176

Aziz, S. G. G., & Almasi, H. (2018). Physical characteristics, release properties, and antioxidant and antimicrobial activities of whey protein isolate films incorporated with thyme (*Thymus vulgaris* L.) extract-loaded nanoliposomes. *Food and Bioprocess Technology*, *11*(8), 1552–1565. https://doi.org/10.1007/s11947-018-2121-6

Błaszczyk, A., Augustyniak, A., & Skolimowski, J. (2013). Ethoxyquin: An antioxidant used in animal feed. *International journal of food science*. https://doi.org/10.1155/2013/585931

Buendía-Moreno, L., Ros-Chumillas, M., Navarro-Segura, L., Sánchez-Martínez, M. J., Soto-Jover, S., Antolinos, V., Martínez-Hernández, G. B., & López-Gómez, A. (2019). Effects of an active cardboard box using encapsulated essential oils on the tomato shelf life. *Food and Bioprocess Technology, 12*(9), 1548–1558. https://doi.org/10.1007/s11947-019-02311-0

Burt, S. (2004). Essential oils: Their antibacterial properties and potential applications in foods—a review. *International Journal of Food Microbiology, 94*(3), 223–253. https://doi.org/10.1016/j.ijfoodmicro.2004.03.022

Cai, M., Wang, Y., Wang, R., Li, M., Zhang, W., Yu, J., & Hua, R. (2022). Antibacterial and antibiofilm activities of chitosan nanoparticles loaded with *Ocimum basilicum* L. essential oil. *International Journal of Biological Macromolecules*. https://doi.org/10.1016/j.ijbiomac.2022.01.066

Cai, R., Hu, M., Zhang, Y., Niu, C., Yue, T., Yuan, Y., & Wang, Z. (2019). Antifungal activity and mechanism of citral, limonene and eugenol against Zygosaccharomyces rouxii. *Lwt, 106*, 50–56. https://doi.org/10.1016/j.lwt.2019.02.059

Chaudhari, A. K., Singh, V. K., Das S, & Dubey, N. K. (2022). Fabrication, characterization, and bioactivity assessment of chitosan nanoemulsion containing allspice essential oil to mitigate *Aspergillus flavus* contamination and aflatoxin B1 production in maize. *Food Chemistry*, *372*,131221. https://doi.org/10.1016/j.foodchem.2021.131221

Chaudhari, A. K., Singh, V. K., Das, S., Singh, B. K., & Dubey, N. K. (2020). Antimicrobial, aflatoxin B1 inhibitory and lipid oxidation suppressing potential of anethole-based chitosan nanoemulsion as novel preservative for protection of stored maize. *Food and Bioprocess Technology, 13*(8), 1462–1477. https://doi.org/10.1007/s11947-020-02479-w

Chen, Z. Y., Brown, R. L., Damann, K. E., & Cleveland, T. E. (2004). Identification of a maize kernel stress-related protein and its effect on aflatoxin accumulation. *Phytopathology, 94*(9), 938–945. https://doi.org/10.1094/PHYTO.2004.94.9.938

Choi, J. H., Nah, J. Y., Lee, M. J., Jang, J. Y., Lee, T., & Kim, J. (2021). Fusarium diversity and mycotoxin occurrence in proso millet in Korea. *LWT*, *141*, 110964. https://doi.org/10.1016/j.lwt.2021.110964

Coates, J. (2000). Interpretation of infrared spectra, a practical approach.

Coats, J. R. (1994). Risks from natural versus synthetic insecticides. *Annual Review of Entomology, 39*(1), 489–515.

da Silva, V. D., Almeida-Souza, F., Teles, A. M., Neto, P. A., Mondego-Oliveira, R., Mendes Filho, N. E., ... & Mouchrek Filho, V. E. (2018). Chemical composition of *Ocimum canum* Sims. essential oil and the antimicrobial, antiprotozoal and ultrastructural alterations it induces in Leishmania amazonensis promastigotes. *Industrial Crops and Products*, *119*, 201–208. https://doi.org/10.1016/j.indcrop.2018.04.005

Danh, L. T., Han, L. N., Triet, N. D. A., Zhao, J., Mammucari, R., & Foster, N. (2013). Comparison of chemical composition, antioxidant and antimicrobial activity of lavender (*Lavandula angustifolia* L.) essential oils extracted by supercritical CO2, hexane and hydrodistillation. *Food and bioprocess technology*, *6*(12), 3481–3489. https://doi.org/10.1007/s11947-012-1026-z

Das, S., Singh, V. K., Dwivedy, A. K., Chaudhari, A. K., & Dubey, N. K. (2020). *Myristica fragrans* essential oil nanoemulsion as novel green preservative against fungal and aflatoxin contamination of food commodities with emphasis on biochemical mode of action and molecular docking of major components. *LWT*, *130*, 109495. https://doi.org/10.1016/j.lwt.2020.109495

Das, S., Singh, V. K., Dwivedy, A. K., Chaudhari, A. K., & Dubey, N. K. (2021a). Insecticidal and fungicidal efficacy of essential oils and nanoencapsulation approaches for the development of next generation ecofriendly green preservatives for management of

stored food commodities: An overview. *International Journal of Pest Management*, 1–32. https://doi.org/10.1080/09670874.2021.1969473

Das, S., Singh, V. K., Dwivedy, A. K., Chaudhari, A. K., & Dubey, N. K. (2021b). Eugenol loaded chitosan nanoemulsion for food protection and inhibition of Aflatoxin B1 synthesizing genes based on molecular docking. *Carbohydrate Polymers, 255*,117339. https://doi.org/10.1016/j.carbpol.2020.117339

Das, S., Singh, V. K., Dwivedy, A. K., Chaudhari, A. K., & Dubey, N. K. (2021c). Anethum graveolens essential oil encapsulation in chitosan nanomatrix: investigations on in-vitro release behaviour, organoleptic attributes, and efficacy as potential delivery vehicles against biodeterioration of rice (*Oryza sativa* L.). *Food and Bioprocess Technology*, *14*(5), 831–853. https://doi.org/10.1007/s11947-021-02589-z

Das, S., Singh, V. K., Dwivedy, A. K., Chaudhari, A. K., & Dubey, N. K. (2021d). Nanostructured *Pimpinella anisum* essential oil as novel green food preservative against fungal infestation, aflatoxin B1 contamination and deterioration of nutritional qualities. *Food Chemistry, 344*, 128574. https://doi.org/10.1016/j.foodchem.2020.128574

de Souza, H. J. B., de Barros Fernandes, R. V., Borges, S. V., Felix, P. H. C., Viana, L. C., Lago, A. M. T., & Botrel, D. A. (2018). Utility of blended polymeric formulations containing cellulose nanofibrils for encapsulation and controlled release of sweet orange essential oil. *Food and Bioprocess Technology, 11*(6), 1188–1198. https://doi.org/10.1007/s11947-018-2082-9

Deepika, Chaudhari, A. K., Singh, A., Das, S., & Dubey, N. K. (2021). Nanoencapsulated *Petroselinum crispum* essential oil: Characterization and practical efficacy against fungal and aflatoxin contamination of stored chia seeds. *Food Bioscience*, *42*, 101117. https://doi.org/10.1016/j.fbio.2021.101117

Dwivedy, A. K., Singh, V. K., Prakash, B., & Dubey, N. K. (2018). Nanoencapsulated Illicium verum Hook. f. essential oil as an effective novel plant-based preservative against aflatoxin B1 production and free radical generation. *Food and Chemical Toxicology*, *111*, 102–113. https://doi.org/10.1016/j.fct.2017.11.007

EFSA Panel on Food Additives and Nutrient Sources added to Food (ANS). (2012). Scientific opinion on the re-evaluation of butylated hydroxytoluene BHT (E 321) as a food additive. *EFSA Journal, 10*(3), 2588. https://doi.org/10.2903/j.efsa.2012.2588

Elsaied, B. E., & Tayel, A. A. (2022). Chitosan-based nanoparticles and their applications in food industry. *Nanotechnology-Enhanced Food Packaging*, 87–128. https://doi.org/10.1002/9783527827718.ch5

Esmaeili, A., & Asgari, A. (2015). In-vitro release and biological activities of *Carum copticum* essential oil (CEO) loaded chitosan nanoparticles. *International Journal of Biological Macromolecules, 81*, 283–290. https://doi.org/10.1016/j.ijbiomac.2015.08.010

Fabra, M. J., Flores-López, M. L., Cerqueira, M. A., de Rodriguez, D. J., Lagaron, J. M., & Vicente, A. A. (2016). Layer-by-layer technique to developing functional nanolaminate films with antifungal activity. *Food and Bioprocess Technology, 9*(3), 471–480. https://doi.org/10.1007/s11947-015-1646-1

Finney, D. J. (1971). *Probit analysis*. Cambridge University Press.

Ghaderi-Ghahfarokhi, M., Barzegar, M., Sahari, M. A., & Azizi, M. H. (2016). Nanoencapsulation approach to improve antimicrobial and antioxidant activity of thyme essential oil in beef burgers during refrigerated storage. *Food and Bioprocess Technology, 9*(7), 1187–1201. https://doi.org/10.1007/s11947-016-1708-z

Gholivand, M. B., Rahimi-Nasrabadi, M., Batooli, H., & Ebrahimabadi, A. H. (2010). Chemical composition and antioxidant activities of the essential oil and methanol extracts of *Psammogeton canescens*. *Food and Chemical Toxicology, 48*(1), 24–28. https://doi.org/10.1016/j.fct.2009.09.007

Giri, P. (2019). Phytochemical Analysis of *Ocimum americanum* Linn. with Special Reference to the Impact of In vitro Flowering on the Production of Aromatic Compounds. *Journal of Biological and chemical Chronicles*, *5*(1), 38–42.

Hadidi, M., Pouramin, S., Adinepour, F., Haghani, S., & Jafari, S. M. (2020). Chitosan nanoparticles loaded with clove essential oil: Characterization, antioxidant and antibacterial activities. *Carbohydrate polymers*, *236*, 116075. https://doi.org/10.1016/j.carbpol.2020.116075

Hariharan, D., Saied, A., & Kocher, H. M. (2008). Analysis of mortality rates for pancreatic cancer across the world. *Hpb*, *10*(1), 58–62. https://doi.org/10.1080/13651820701883148

Hasheminejad, N., Khodaiyan, F., & Safari, M. (2019). Improving the antifungal activity of clove essential oil encapsulated by chitosan nanoparticles. *Food Chemistry, 275*, 113–122. https://doi.org/10.1016/j.foodchem.2018.09.085

Hassane, S. O. S., Farah, A., Satrani, B., Ghanmi, M., Chahmi, N., Soidrou, S. H., & Chaouch, A. (2012). Chemical composition and antimicrobial activity of comorian *Ocimum canum* essential oil harvested in the region of Maweni Dimani-Grande Comoros. In *Chemistry for sustainable development* (pp. 443–452). Springer, Dordrecht. https://doi.org/10.1007/978-90-481-8650-1_29

Hemmatkhah, F., Zeynali, F., & Almasi, H. (2020). Encapsulated cumin seed essential oil-loaded active papers: Characterization and evaluation of the effect on quality attributes of beef hamburger. *Food and Bioprocess Technology, 13*(3), 533–547. https://doi.org/10.1007/s11947-020-02418-9

Hosseini, S. F., Zandi, M., Rezaei, M., & Farahmandghavi, F. (2013). Two-step method for encapsulation of oregano essential oil in chitosan nanoparticles: Preparation, characterization and in vitro release study. *Carbohydrate Polymers, 95*(1), 50–56. https://doi.org/10.1016/j.carbpol.2013.02.031

Hussain, A. I., Anwar, F., Sherazi, S. T. H., & Przybylski, R. (2008). Chemical composition, antioxidant and antimicrobial activities of basil (*Ocimum basilicum*) essential oils depends on seasonal variations. *Food Chemistry, 108*(3), 986–995. https://doi.org/10.1016/j.foodchem.2007.12.010

International Agency for Research on Cancer. (2012). A review of human carcinogens. F. Chemical Agents and Related Occupations: IARC Monographs on the Evaluation of Carcinogenic Risks to Humans.

Isman, M. B. (2006). Botanical insecticides, deterrents, and repellents in modern agriculture and an increasingly regulated world. *Annual Review of Entomology, 51*, 45–66. https://doi.org/10.1146/annurev.ento.51.110104.151146

Jafarzadeh, S., Hadidi, M., Forough, M., Nafchi, A. M., & Mousavi Khaneghah, A. (2022). The control of fungi and mycotoxins by food active packaging: A review. *Critical Reviews in Food Science and Nutrition*, 1–19. https://doi.org/10.1080/10408398.2022.2031099

Ju, J., Xie, Y., Yu, H., Guo, Y., Cheng, Y., Zhang, R., & Yao, W. (2020). Synergistic inhibition effect of citral and eugenol against *Aspergillus niger* and their application in bread preservation. *Food Chemistry*, *310*, 125974. https://doi.org/10.1016/j.foodchem.2019.125974

Kedia, A., Prakash, B., Mishra, P. K., & Dubey, N. K. (2014). Antifungal and antiaflatoxigenic properties of *Cuminum cyminum* (L.) seed essential oil and its efficacy as a preservative in stored commodities. *International Journal of Food Microbiology, 168*, 1–7. https://doi.org/10.1016/j.ijfoodmicro.2013.10.008

Kola, G., Reddy, P. C. O., Shaik, S., Gunti, M., Palakurthi, R., Talwar, H. S., & Sekhar, A. C. (2020). Variability in seed mineral composition of foxtail millet (*Setaria italica* L.) landraces and released cultivars. *Current Trends in Biotechnology & Pharmacy*, 10. https://doi.org/10.5530/ctbp.2020.3.25

Kos, J., Hajnal, E. J., Malachová, A., Steiner, D., Stranska, M., Krska, R., & Sulyok, M. (2020). Mycotoxins in maize harvested in Republic of Serbia in the period 2012–2015. Part 1: Regulated mycotoxins and its derivatives. *Food chemistry*, *312*, 126034. https://doi.org/10.1016/j.foodchem.2019.126034

Kujur, A., Kumar, A., Singh, P. P., & Prakash, B. (2021). Fabrication, characterization, and antifungal assessment of Jasmine essential oil-loaded chitosan nanomatrix against Aspergillus flavus in food system. *Food and Bioprocess Technology, 14*(3), 554–571. https://doi.org/10.1007/s11947-021-02592-4

Lai, T. Y., Chen, C. H., & Lai, L. S. (2013). Effects of tapioca starch/decolorized hsian-tsao leaf gum-based active coatings on the quality of minimally processed carrots. *Food and Bioprocess Technology, 6*(1), 249–258. https://doi.org/10.1007/s11947-011-0707-3

Lata, C., Gupta, S., & Prasad, M. (2013). Foxtail millet: A model crop for genetic and genomic studies in bioenergy grasses. *Critical Reviews in Biotechnology, 33*(3), 328–343. https://doi.org/10.3109/07388551.2012.716809

Lee, J. J. L., Cui, X., Chai, K. F., Zhao, G., & Chen, W. N. (2020). Interfacial assembly of a cashew nut (Anacardium occidentale) testa extract onto a cellulose-based film from sugarcane bagasse to produce an active packaging film with pH-triggered release mechanism. *Food and Bioprocess Technology, 13*(3), 501–510. https://doi.org/10.1007/s11947-020-02414-z

López-Meneses, A. K., Plascencia-Jatomea, M., Lizardi-Mendoza, J., Fernández-Quiroz, D., Rodríguez-Félix, F., Mouriño-Pérez, R. R., & Cortez-Rocha, M. O. (2018). *Schinus molle* L. essential oil-loaded chitosan nanoparticles: Preparation, characterization, antifungal and anti-aflatoxigenic properties. *LWT, 96*, 597–603. https://doi.org/10.1016/j.lwt.2018.06.013

Maleki, G., Woltering, E. J., & Mozafari, M. R. (2022). Applications of chitosan-based carrier as an encapsulating agent in food industry. *Trends in Food Science & Technology*. https://doi.org/10.1016/j.tifs.2022.01.001

Matasyoh, J. C., Bendera, M. M., Ogendo, J. O., Omollo, E. O., & Deng, A. L. (2006). Volatile leaf oil constituents of *Ocimum americanum* L. occuring in Western Kenya. *Bulletin of the Chemical Society of Ethiopia*, *20*(1), 177–180. https://doi.org/10.4314/bcse.v20i1.21159

Matshetshe, K. I., Parani, S., Manki, S. M., & Oluwafemi, O. S. (2018). Preparation, characterization and in vitro release study of β-cyclodextrin/chitosan nanoparticles loaded Cinnamomum zeylanicum essential oil. *International Journal of Biological Macromolecules, 118*, 676–682. https://doi.org/10.1016/j.ijbiomac.2018.06.125

Nada, S., Nikola, T., Bozidar, U., Ilija, D., & Andreja, R. (2022). Prevention and practical strategies to control mycotoxins in the wheat and maize chain. *Food Control*, 108855. https://doi.org/10.1016/j.foodcont.2022.108855

Navikaite-Snipaitiene, V., Ivanauskas, L., Jakstas, V., Rüegg, N., Rutkaite, R., Wolfram, E., & Yildirim, S. (2018). Development of antioxidant food packaging materials containing eugenol for extending display life of fresh beef. *Meat Science, 145*, 9–15. https://doi.org/10.1016/j.meatsci.2018.05.015

Ostry, V., Malir, F., Toman, J., & Grosse, Y. (2017). Mycotoxins as human carcinogens—The IARC Monographs classification. *Mycotoxin Research, 33*(1), 65–73. https://doi.org/10.1007/s12550-016-0265-7

OuYang, Q., Okwong, R. O., Chen, Y., & Tao, N. (2020). Synergistic activity of cinnamaldehyde and citronellal against green mold in citrus fruit. *Postharvest Biology and Technology*, *162*, 111095. https://doi.org/10.1016/j.postharvbio.2019.111095

Pabast, M., Shariatifar, N., Beikzadeh, S., & Jahed, G. (2018). Effects of chitosan coatings incorporating with free or nano-encapsulated *Satureja* plant essential oil on quality characteristics of lamb meat. *Food Control, 91*, 185–192. https://doi.org/10.1016/j.foodcont.2018.03.047

Panda, P. K., Yang, J. M., Chang, Y. H., & Su, W. W. (2019). Modification of different molecular weights of chitosan by p-Coumaric acid: Preparation, characterization and effect of molecular weight on its water solubility and antioxidant property. *International Journal of Biological Macromolecules, 136*, 661–667. https://doi.org/10.1016/j.ijbiomac.2019.06.082

Papoutsis, K., Mathioudakis, M. M., Hasperué, J. H., & Ziogas, V. (2019). Non-chemical treatments for preventing the postharvest fungal rotting of citrus caused by *Penicillium digitatum* (green mold) and *Penicillium italicum* (blue mold). *Trends in Food Science & Technology, 86*, 479–491. https://doi.org/10.1016/j.tifs.2019.02.053

Peretto, G., Du, W. X., Avena-Bustillos, R. J., De J. Berrios, J., Sambo, P., & McHugh, T. H. (2017). Electrostatic and conventional spraying of alginate-based edible coating with natural antimicrobials for preserving fresh strawberry quality. *Food and Bioprocess Technology*, *10*, 165–174. https://doi.org/10.1007/s11947-016-1808-9

Plati, F., & Paraskevopoulou, A. (2022). Micro-and nano-encapsulation as tools for essential oils advantages' exploitation in food applications: The case of oregano essential oil. *Food and Bioprocess Technology*, 1–29. https://doi.org/10.1007/s11947-021-02746-4

Prasad, J., Das, S., Maurya, A., Jain, S. K., & Dwivedy, A. K. (2022). Synthesis, characterization and in situ bioefficacy evaluation of *Cymbopogon nardus* essential oil impregnated chitosan nanoemulsion against fungal infestation and aflatoxin B1 contamination in food system. *International Journal of Biological Macromolecules*. https://doi.org/10.1016/j.ijbiomac.2022.02.060

Re, R., Pellegrini, N., Proteggente, A., Pannala, A., Yang, M., & Rice-Evans, C. (1999). Antioxidant activity applying an improved ABTS radical cation decolorization assay. *Free Radical Biology and Medicine, 26*(9–10), 1231–1237. https://doi.org/10.1016/S0891-5849(98)00315-3

Roshan, A. B., Dubey, N. K., & Mohana, D. C. (2021). Chitosan nanoencapsulation of Pogostemon cablin (Blanco) Benth. essential oil and its novel preservative effect for enhanced shelf life of stored Maize kernels during storage: Evaluation of its enhanced antifungal, antimycotoxin, antioxidant activities and possible mode of action. *International Journal of Food Science & Technology*. https://doi.org/10.1111/ijfs.15289

Roshan, A. B., Venkatesh, H. N., Dubey, N. K., & Mohana, D. C. (2022). Chitosan-based nanoencapsulation of *Toddalia asiatica* (L.) Lam. essential oil to enhance antifungal and aflatoxin B1 inhibitory activities for safe storage of maize. *International Journal of Biological Macromolecules, 204*, 476–484. https://doi.org/10.1016/j.ijbiomac.2022.02.026

Saeed, K., Pasha, I., Jahangir Chughtai, M. F., Ali, Z., Bukhari, H., & Zuhair, M. (2022). Application of essential oils in food industry: challenges and innovation. *Journal of Essential Oil Research*, 1–14. https://doi.org/10.1080/10412905.2022.2029776

Sarin, Y. K., Agarwal, S. G., Thappa, R. K., Singh, K., & Kapahi, B. K. (1992). A high yielding citral-rich strain of *Ocimum americanum* L. from India. *Journal of Essential Oil Research*, *4*(5), 515–519. https://doi.org/10.1080/10412905.1992.9698119

Sarma, D. S. K., & Babu, A. V. S. (2011). Pharmacognostic and phytochemical studies of *Ocimum americanum*. *Journal of Chemical and Pharmaceutical Research, 3*(3), 337–347.

Shadia, E., El-Aziz, A. B. D., Omer, E. A., & Sabra, A. S. (2007). Chemical composition of *Ocimum americanum* essential oil and its biological effects against *Agrotis ipsilon* (Lepidoptera: Noctuidae). *Research Journal of Agriculture and Biological Sciences, 3*(6), 740–747.

Sharma, N., & Niranjan, K. (2018). Foxtail millet: Properties, processing, health benefits, and uses. *Food Reviews International, 34*(4), 329–363. https://doi.org/10.1080/87559129.2017.1290103

Simon, J. E., Morales, M. R., Phippen, W. B., Vieira, R. F., & Hao, Z. (1999). Basil: A source of aroma compounds and a popular culinary and ornamental herb. *Perspectives on New Crops and New Uses, 16*, 499–505.

Singh, B. K., Tiwari, S., & Dubey, N. K. (2021). Essential oils and their nanoformulations as green preservatives to boost food

safety against mycotoxin contamination of food commodities: A review. *Journal of the Science of Food and Agriculture, 101*(12), 4879–4890. https://doi.org/10.1002/jsfa.11255

Singh, B. K., Tiwari, S., Maurya, A., Kumar, S., & Dubey, N. K. (2022). Fungal and mycotoxin contamination of herbal raw materials and their protection by nanoencapsulated essential oils: An overview. *Biocatalysis and Agricultural Biotechnology*, *39*, 102257. https://doi.org/10.1016/j.bcab.2021.102257

Singh, P. P., Kumar, A., & Prakash, B. (2020). Elucidation of antifungal toxicity of *Callistemon lanceolatus* essential oil encapsulated in chitosan nanogel against *Aspergillus flavus* using biochemical and in-silico approaches. *Food Additives & Contaminants: Part A, 37*(9), 1520–1530. https://doi.org/10.1080/19440049.2020.1775310

Singh, V., Praveen, V., Tripathi, D., Haque, S., Somvanshi, P., Katti, S. B., & Tripathi, C. K. M. (2015). Isolation, characterization and antifungal docking studies of wortmannin isolated from *Penicillium radicum*. *Scientific Reports, 5*(1), 1–13. https://doi.org/10.1038/srep11948

Souza, M. P., Vaz, A. F., Cerqueira, M. A., Texeira, J. A., Vicente, A. A., & Carneiro-da-Cunha, M. G. (2015). Effect of an edible nanomultilayer coating by electrostatic self-assembly on the shelf life of fresh-cut mangoes. *Food and Bioprocess Technology, 8*(3), 647–654. https://doi.org/10.1007/s11947-014-1436-1

Tavassoli-Kafrani, E., Goli, S. A. H., & Fathi, M. (2018). Encapsulation of orange essential oil using cross-linked electrospun gelatin nanofibers. *Food and Bioprocess Technology, 11*(2), 427–434. https://doi.org/10.1007/s11947-017-2026-9

Tian, J., Huang, B., Luo, X., Zeng, H., Ban, X., He, J., & Wang, Y. (2012). The control of Aspergillus flavus with *Cinnamomum jensenianum* Hand.-Mazz essential oil and its potential use as a food preservative. *Food Chemistry*, *130*(3), 520–527. https://doi.org/10.1016/j.foodchem.2011.07.061

Tiwari, S., Upadhyay, N., Singh, B. K., Singh, V. K., & Dubey, N. K. (2022a). Facile fabrication of nanoformulated *Cinnamomum glaucescens* essential oil as a novel green strategy to boost potency against food borne fungi, aflatoxin synthesis, and lipid oxidation. *Food and Bioprocess Technology*, 1–19. https://doi.org/10.1007/s11947-021-02739-3

Tiwari, S., Upadhyay, N., Singh, B. K., Singh, V. K., & Dubey, N. K. (2022b). Chemically characterized nanoencapsulated *Homalomena aromatica* Schott. essential oil as green preservative against fungal and aflatoxin B1 contamination of stored spices based on in vitro and in situ efficacy and favorable safety profile on mice. *Environmental Science and Pollution Research*, *29*(2), 3091–3106. https://doi.org/10.1007/s11356-021-15794-2

Udeh, H. O., & Kgatla, T. E. (2013). Role of magnesium ions on yeast performance during very high gravity fermentation. *Journal of Brewing and Distilling, 4*(2), 19–45. https://doi.org/10.5897/JBD2013.0041

Upadhyay, N., Singh, V. K., Dwivedy, A. K., Chaudhari, A. K., & Dubey, N. K. (2021). Assessment of nanoencapsulated Cananga odorata essential oil in chitosan nanopolymer as a green approach to boost the antifungal, antioxidant and in situ efficacy. *International Journal of Biological Macromolecules, 171*, 480–490. https://doi.org/10.1016/j.ijbiomac.2021.01.024

Upadhyay, N., Singh, V. K., Dwivedy, A. K., Das, S., Chaudhari, A. K., & Dubey, N. K. (2018). *Cistus ladanifer* L. essential oil as a plant-based preservative against molds infesting oil seeds, aflatoxin B1 secretion, oxidative deterioration and methylglyoxal biosynthesis. *LWT-Food Science and Technology, 92*, 395–403. https://doi.org/10.1016/j.lwt.2018.02.040

Verma, R. S., Kumar, A., Mishra, P., Kuppusamy, B., Padalia, R. C., & Sundaresan, V. (2016). Essential oil composition of four *Ocimum* spp. from the Peninsular India**.** *Journal of Essential Oil Research*, *28*(1), 35–41. https://doi.org/10.1080/10412905.2015.1076742

Wani, H. M., Sharma, P., Wani, I. A., Kothari, S. L., & Wani, A. A. (2021). Influence of γ-irradiation on antioxidant, thermal and rheological properties of native and irradiated whole grain millet flours. *International Journal of Food Science & Technology, 56*(8), 3752–3762. https://doi.org/10.1111/ijfs.15062

Wani, T. A., Masoodi, F. A., Akhter, R., Akram, T., Gani, A., & Shabir, N. (2022). Nanoencapsulation of hydroxytyrosol in chitosan crosslinked with sodium bisulfate tandem ultrasonication: Techno-characterization, release and antiproliferative properties. *Ultrasonics Sonochemistry*, *82*, 105900. https://doi.org/10.1016/j.ultsonch.2021.105900

Woranuch, S., & Yoksan, R. (2013). Preparation, characterization and antioxidant property of water-soluble ferulic acid grafted chitosan. *Carbohydrate Polymers, 96*(2), 495–502. https://doi.org/10.1016/j.carbpol.2013.04.006

Xing, F., Wang, L., Liu, X., Selvaraj, J. N., Wang, Y., Zhao, Y., & Liu, Y. (2017). Aflatoxin B1 inhibition in *Aspergillus flavus* by *Aspergillus niger* through down-regulating expression of major biosynthetic genes and AFB1 degradation by atoxigenic A. flavus. *International Journal of Food Microbiology, 256*, 1–10. https://doi.org/10.1016/j.ijfoodmicro.2017.05.013

Xu, D., Wei, M., Peng, S., Mo, H., Huang, L., Yao, L., & Hu, L. (2021). Cuminaldehyde in cumin essential oils prevents the growth and aflatoxin B1 biosynthesis of Aspergillus flavus in peanuts. *Food Control*, *125*, 107985. https://doi.org/10.1016/j.foodcont.2021.107985

Yadav, S. K., Singla-Pareek, S. L., Ray, M., Reddy, M. K., & Sopory, S. K. (2005). Methylglyoxal levels in plants under salinity stress are dependent on glyoxalase I and glutathione. *Biochemical and Biophysical Research Communications, 337*(1), 61–67. https://doi.org/10.1016/j.bbrc.2005.08.263

Yamada, A. N., Grespan, R., Yamada, Á. T., Silva, E. L., Silva-Filho, S. E., Damião, M. J., ... & Cuman, R. K. N. (2013). Anti-inflammatory activity of *Ocimum americanum* L. essential oil in experimental model of zymosan-induced arthritis. *The American Journal of Chinese Medicine*, *41*(04), 913–926. https://doi.org/10.1142/S0192415X13500614

Yang, T., Qin, W., Zhang, Q., Luo, J., Lin, D., & Chen, H. (2022). Essential-oil capsule preparation and its application in food preservation: A review. *Food Reviews International*, 1–35. https://doi.org/10.1080/87559129.2021.2021934

Yoksan, R., Jirawutthiwongchai, J., & Arpo, K. (2010). Encapsulation of ascorbyl palmitate in chitosan nanoparticles by oil-in-water emulsion and ionic gelation processes. *Colloids and Surfaces B: Biointerfaces, 76*(1), 292–297. https://doi.org/10.1016/j.colsurfb.2009.11.007

Zargar, V., Asghari, M., & Dashti, A. (2015). A review on chitin and chitosan polymers: Structure, chemistry, solubility, derivatives, and applications. *ChemBioEng Reviews, 2*(3), 204–226. https://doi.org/10.1002/cben.201400025

Zhu, D., Guo, R., Li, W., Song, J., & Cheng, F. (2019). Improved postharvest preservation effects of Pholiota nameko mushroom by sodium alginate–based edible composite coating. *Food and Bioprocess Technology, 12*(4), 587–598. https://doi.org/10.1007/s11947-019-2235-5